Summer 7-1-1985

Cross Polarization Level in Radiation from a Microstrip Dipole Antenna

Ahmad Hoorfar
University of Colorado Boulder

K C. Gupta
University of Colorado Boulder

David C. Chang
University of Colorado Boulder

SCIENTIFIC REPORT NO. 83

CROSS-POLARIZATION LEVEL IN RADIATION FROM A MICROSTRIP DIPOLE ANTENNA

by

Ahmad Hoorfar, K.C. Gupta, and D.C. Chang

Electromagnetics Laboratory
Department of Electrical and Computer Engineering
Campus Box 425
University of Colorado
Boulder, Colorado

July 1985

This work has been supported by the Department of the Navy

under Contract # NAVYN60530841.CO095

Abstract

Cross-polarization level, inherent in radiation from a small horizontal electric dipole (HED) on a flat grounded dielectric substrate, is investigated in detail. The study is directed towards the design of a very low cross-pol level in a linear array of microstrip antenna elements. Field expressions for a microstrip HED are derived in spherical coordinates with respect to the array direction. In particular, two important cases, namely a HED along the array direction (i.e., parallel polarization) and a HED perpendicular to array direction (i.e., perpendicular polarization) are investigated. Extensive numerical examples for the cross-pol levels are given. It is shown that, in general, there are inherent limitations in achieving very low cross-pol levels, especially for the case of parallel polarization.

Table of Contents

List of Figures

Fig. 12: CPL for a Y-directed HED as a function of k_0d; $\epsilon_r = 2$, $\theta_y = 50°, 60°, 70°$, and $80°$.

Fig. 13: Co-pol and cross-pol radiation patterns for a X-directed HED; $\theta_y = 60°$, $\epsilon_r = 2$, $k_0d = 0.1$.

Fig. 14: Co-polar and cross-pol radiation patterns for a X-directed HED; $\theta_y = 60°$, $\epsilon_r = 2$, $k_0d = 0.5$.

Fig. 15: Co-pol and cross-pol radiation patterns for a X-directed HED; $\theta_y = 60°$, $\epsilon_r = 10$, $k_0d = 0.1$.

Fig. 16: CPL for a X-directed HED as a function of $\sqrt{\epsilon_r}\, k_0d$; $\theta_y = 50°$, $\epsilon_r = 2, 5$, and 10.

Fig. 17: CPL for a X-directed HED as a function of $\sqrt{\epsilon_r}\, k_0d$; $\theta_y = 60°$, $\epsilon_r = 2, 5$, and 10.

Fig. 18: CPL for a X-directed HED as a function of $\sqrt{\epsilon_r}\, k_0d$; $\theta_y = 70°$, $\epsilon_r = 2, 5$, and 10.

Fig. 19: CPL for a X-directed HED as a function of $\sqrt{\epsilon_r}\, k_0d$; $\theta_y = 80°$, $\epsilon_r = 2, 5$, and 10.

Fig. 20: CPL for a X-directed HED as a function of k_0d; $\epsilon_r = 2$, $\theta_y = 50°, 60°, 70°$, and $80°$.

1. Introduction

Examination of the possibility of obtaining a -30 dB cross-polarization level in a linear array of microstrip antenna elements motivated the work described in this report. Since the cross-polar side lobes in directions other than that of the beam are reduced by array factor, the cross-polarization level in the direction of the beam is the dominant in calculation of the cross-polar side lobes (i.e., cross-pol level) of a linear array. In the present case, the direction of the beam is assumed to be between 10° to 40° from broadside.

This report describes the investigations of the cross-pol level inherent in the radiation from a small, arbitrarily-oriented, horizontal electric current element on a flat grounded dielectric substrate (Figure 1). Usually, coordinate system selected for deriving the fields of a current element has the z-axis (i.e., reference axis of the spherical coordinate (r, θ_z, ϕ_z)), normal to the substrate [for example, see 1] as seen in Figures 1 and 2. However, for the linear array problem, it is desirable to use a polar coordinate system with reference axis along the array axis, say, the y-axis (Figure 3). This choice of the polar direction, makes it convenient to evaluate co-polar and cross-polar fields with respect to the beam direction. Thus it is desirable to derive the field expressions for the case when the polar-axis is in the plane of the substrate.

In section 2 of this report, based on a directional-cosine formulation, field expressions for a microstrip horizontal electric dipole (HED) are derived in a spherical coordinate with respect to any arbitrarily-oriented axis. In particular, the field expressions with respect to the y-axis (which is along the array direction) are explicitly given.

In section 3, a definition of the cross-polar side lobe level, according to the IEEE standard [2] is given and two important cases, namely, a y-directed HED (i.e., parallel polarization) and an x-directed HED (i.e., perpendicular polarization) are discussed. Also included in this section are the expressions of co-polar and cross-polar fields for an arbitrarily-oriented HED.

In section 4, numerical examples for the co-polar and cross-polar radiation patterns are given and a parametric study of the cross-pol level (for the two different polarizations) is presented. Finally, in section 5, the results are summarized and inherent limitations in achieving very low cross-pol levels are discussed.

2. Formulation

2.1 Derivation of the Radiated Fields

A horizontal electric dipole (HED) is placed on a grounded dielectric slab as shown in Figure 1. The diople source is of moment p and directed at an angle χ with the x-axis in the x-y plane. The dielectric slab is of thickness d and assumed to be infinitely extended in the x-y plane. As shown in Figure 1, the permittivities in the air and the slab regions are ϵ_0 and ϵ_1, respectively; the permeability in both media is assumed to be μ_0.

To find the field expressions due to this HED current source, we employ the z components of two electric and magnetic Hertz vector potentials, Π_e and Π_m. Outside of the source region (i.e., outside z=0 plane), we have [3],

$$\overline{E} = \nabla \times \nabla \times (\Pi_e \overline{a_z}) + i\,\omega\,\mu_0 \nabla \times (\Pi_m \overline{a_z}) \tag{1.1}$$

$$\overline{H} = \nabla \times \nabla \times (\Pi_m \overline{a_z}) - i\,\omega\,\epsilon \nabla \times (\Pi_e \overline{a_z}) \tag{1.2}$$

The potentials Π_e and Π_m satisfy the homogeneous Helmholtz equation

$$(\nabla^2 + k^2)\,\Pi_{e,m} = 0 \qquad z \neq 0 \tag{2}$$

In (1) and (2), $\epsilon = \epsilon_0$ or ϵ_1 and $k = k_0$ or k_1, depending upon the medium in which the observation point is located.

Equations in (1) can further be reduced to

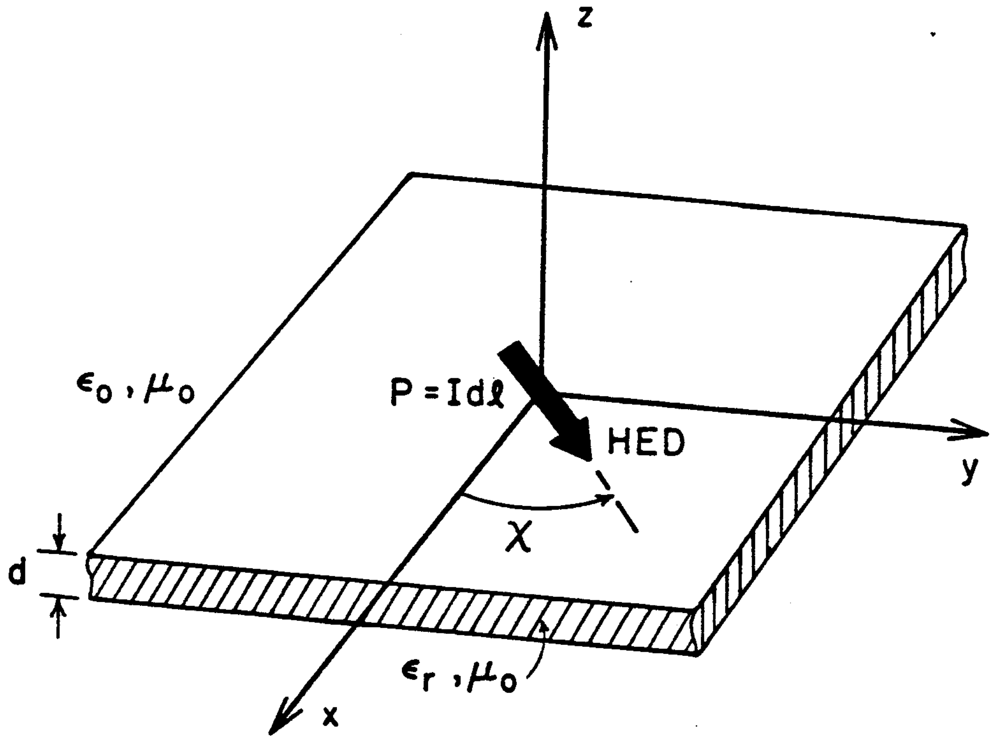

Fig. 1: An arbitrarily-oriented microstrip dipole antenna.

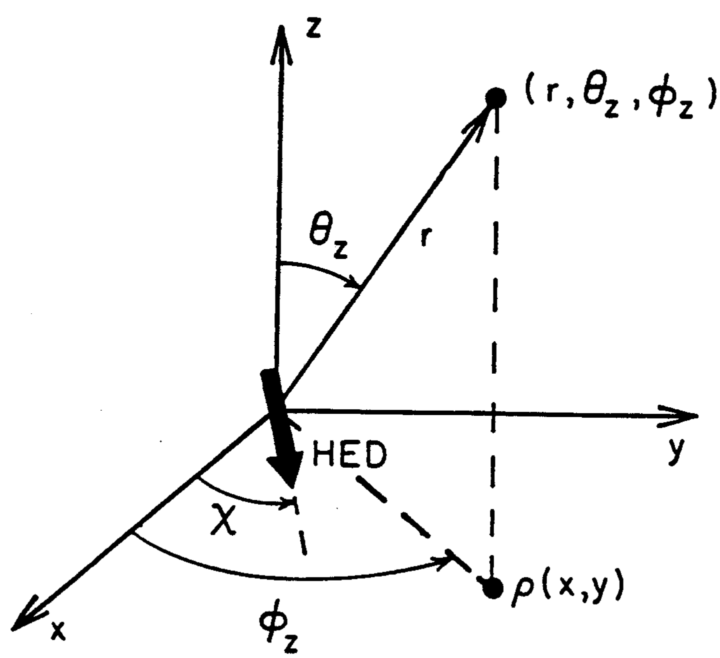

Fig. 2: Spherical coordinate with respect to z -axis.

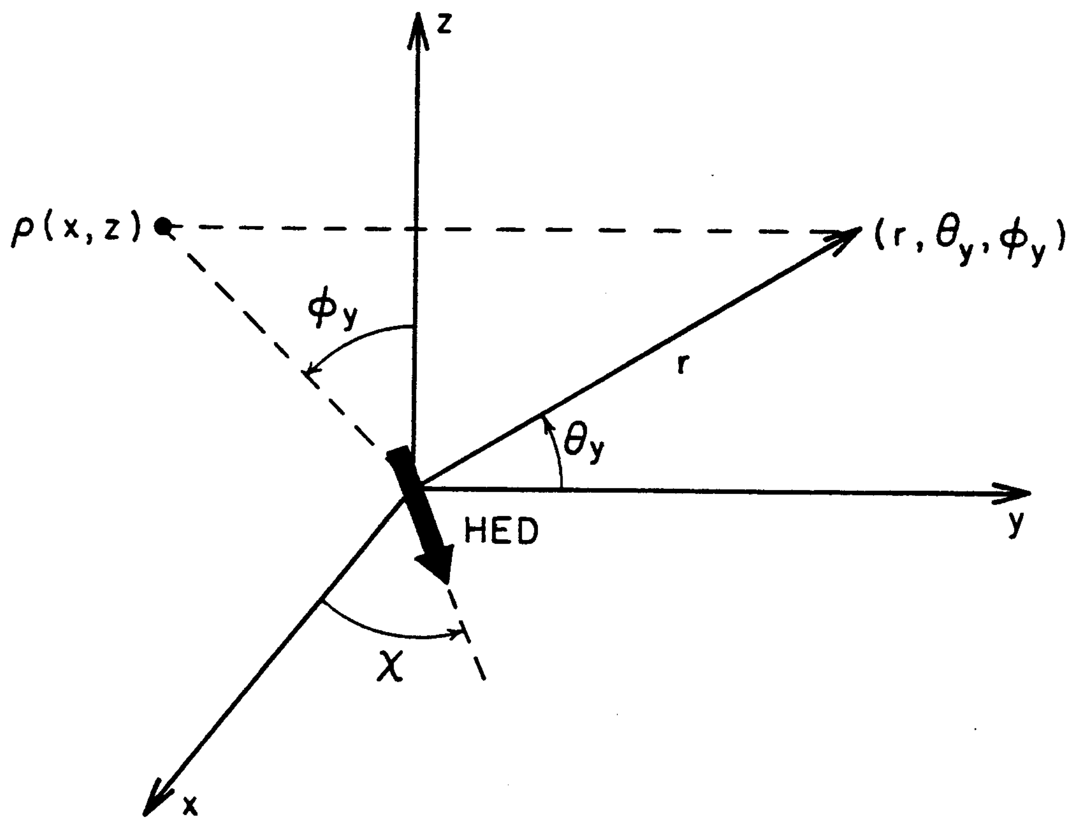

Fig. 3(a): Spherical coordinates with respect to the y-axis.

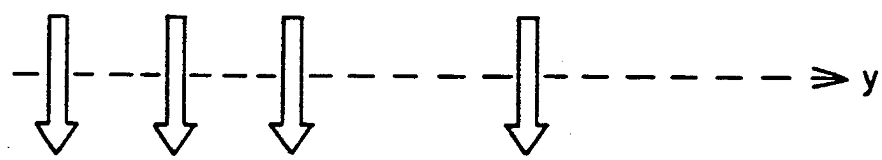

Fig. 3(b): X-directed HED, i.e., polarization perpendicular to array axis.

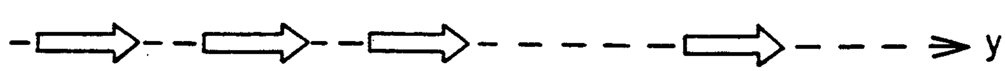

Fig. 3(c): Y-directed HED, i.e., polarization along the array axis.

$$E_z = -\nabla_t^2 \Pi_e \quad ; \quad \bar{E}_t = \nabla_t \frac{\partial \Pi_e}{\partial z} - i\,\omega\,\mu_0\,\bar{a}_z \times \nabla \Pi_m \tag{3.1}$$

$$H_z = -\nabla_t^2 \Pi_m \quad : \quad \bar{H}_t = \nabla_t \frac{\partial \Pi_m}{\partial z} + i\,\omega\,\epsilon\,\bar{a}_z \times \nabla \Pi_e \tag{3.2}$$

where the subscript t denotes to the transverse components with respect to z. Now since

$$\nabla_t \cdot \bar{E}_t = -\frac{\partial}{\partial z} E_z \quad ; \quad \bar{a}_z \cdot \nabla_t \times \bar{E}_t = +\, i\,\omega\,\mu_0\, Hz$$

$$\nabla_t \cdot \bar{H}_t = -\frac{\partial}{\partial z} H_z \quad ; \quad \bar{a}_z \cdot \nabla_t \times \bar{H}_t = -i\,\omega\,\epsilon\, E_z$$

the boundary conditions can be translated into the following conditions for E_z and H_z,

$$H_z|_{z+} = H_z|_{z-} \quad ; \quad E_z'|_{z+} = E_z'|_{z-} \tag{4.1}$$

$$H_z'|_{z+} - H_z'|_{z-} = -\bar{a}_z \cdot \nabla_t \times \bar{J}_s \tag{4.2}$$

$$\frac{ik_0}{\eta_0}\left(E_z|_{z+} - \epsilon_r\, E_z|_{z-}\right) = \nabla_t \cdot \bar{J}_s \tag{4.3}$$

at $z = 0$, and

$$H_z = 0 \quad ; \quad E_z' = 0 \tag{5}$$

at $z = -d$, where η_0 (= 120 π ohms) is the free-space characteristic impedance and ϵ_r (= ϵ_1/ϵ_0) is the refractive index of the dielectric substrate.

To solve equation (2) subject to the boundary conditions in (4) and (5), we first define the Fourier transform pair as:

$$f(x,y) = \int_{-\infty}^{\infty}\int_{-\infty}^{\infty} \tilde{f}(\alpha,\beta)\, e^{-ik_0(\alpha x + \beta y)}\, d\alpha\, d\beta \tag{6.1}$$

$$\tilde{f}(\alpha,\beta) = \left(\frac{k_0}{2\pi}\right)^2 \int_{-\infty}^{\infty}\int_{-\infty}^{\infty} f(x,y)e^{ik_0(\alpha x + \beta y)}\,dx\,dy \; ; \tag{6.2}$$

in transform domain, then, we have,

$$\tilde{\nabla}_t : ik_0(\alpha\,\overline{a}_x + \beta\,\overline{a}_y) \tag{7}$$

$$\tilde{E}_z = k_0^2(\alpha^2 + \beta^2)\tilde{\Pi}_e$$

$$\tilde{H}_z = k_0^2(\alpha^2 + \beta^2)\,\tilde{\Pi}_m$$

where $\tilde{\Pi}_e$ and $\tilde{\Pi}_m$ now satisfy the equation

$$\left(\frac{\partial^2}{\partial z^2} - k_0^2\, U_{0,1}\right)\tilde{\Pi}_{e,m} = 0 \tag{8}$$

wherein

$$U_0 = \sqrt{\alpha^2 + \beta^2 - 1} \; ; \tag{9}$$

$$U_1 = \sqrt{\alpha^2 + \beta^2 - \epsilon_r}$$

$$\mathrm{Re}(U_{0,1}) > 0 \; ; \; \mathrm{Im}(U_{0,1}) < 0$$

From (7), (8) and (5), the solutions for E_z and H_z can be constructed as

$$\begin{cases} \tilde{E}_z = E_1\,\mathrm{ch}\,[U_1 k_0(z + d)] \\ \tilde{H}_z = H_1\,\mathrm{sh}\,[U_1 k_0(z + d)] \end{cases} \tag{10}$$

for $-d < z < 0$, and

$$\begin{pmatrix} \tilde{E}_z \\ \tilde{H}_z \end{pmatrix} = \begin{pmatrix} E_0 \\ H_0 \end{pmatrix} e^{-U_0 k_0 z} \tag{11}$$

for $z > 0$. We now substitute for E_z and H_z from (10) and (11) into (4.1)-(4.3) and solve for the coefficients $E_{0,1}$ and $H_{0,1}$; this finally yields

$$\begin{cases} E_0 = \dfrac{-i\eta_0}{k_0} (\widetilde{\nabla_t \cdot \bar{J}_s}) \dfrac{U_1 \, th(U_1 k_0 d)}{D_{TM}} \\ H_0 = \dfrac{1}{k_0} (\bar{a}_z \cdot \widetilde{\nabla_t \times \bar{J}_s}) \dfrac{1}{D_{TE}} \end{cases} \tag{12}$$

and

$$\begin{cases} E_1 = -\dfrac{U_0}{U_1 \, sh(U_1 k_0 d)} E_0 \\ H_1 = \dfrac{1}{sh(U_1 k_0 d)} H_0 \end{cases} \tag{13}$$

where

$$\begin{aligned} D_{TE} &= U_0 + U_1 \, cth\,(U_1 k_0 d) \\ D_{TM} &= \epsilon_r U_0 + U_1 \, th(U_1 k_0 d) \end{aligned} \tag{14}$$

Equations (10) and (11), via (7) and (6.1), now yield the formal expressions for Π_e and Π_m. In particular, for $z > 0$ one gets

$$\begin{cases} \Pi_e = \dfrac{-i\eta_0}{k_0^3} \displaystyle\int_{-\infty}^{\infty} \int_{-\infty}^{\infty} \dfrac{1}{\alpha^2 + \beta^2} (\widetilde{\nabla_t \cdot \bar{J}_s}) \dfrac{U_1 th(U_1 k_0 d)}{D_{TM}} e^{-U_0 k_0 z} e^{-ik_0(\alpha x + \beta y)} \, d\alpha d\beta \\ \Pi_m = \dfrac{1}{k_0^3} \displaystyle\int_{-\infty}^{\infty} \int_{-\infty}^{\infty} \dfrac{1}{\alpha^2 + \beta^2} (\bar{a}_z \cdot \widetilde{\nabla_t \times \bar{J}_s}) \dfrac{1}{D_{TE}} e^{-U_0 k_0 z} e^{-ik_0(\alpha x + \beta y)} \, d\alpha d\beta \end{cases} \tag{15}$$

It should be noted that the expresions in (15) are valid for any source distribution $\bar{J}_s$ on the slab in the x-y plane. For the present case of a dipole source of moment p which is directed at an angle χ with the x-axis, one can easily show that

$$\widetilde{\nabla_t \cdot \bar{J}_s} = i \frac{k_0^3}{4\pi^2} p\,(\alpha \cos\chi + \beta \sin\chi)$$

$$\bar{a}_z \cdot \widetilde{\nabla_t \times \bar{J}_s} = i \frac{k_0^3}{4\pi^2} p\,(\alpha \sin\chi - \beta \cos\chi)\,,$$

and therefore, for $z > 0$,

$$\begin{cases} \Pi_e = \dfrac{\eta_0 P}{4\pi^2} \displaystyle\int_{-\infty}^{\infty} \int_{-\infty}^{\infty} (\alpha \cos\chi + \beta \sin\chi)\, \tilde{f}_e(U_0)\, e^{-U_0 k_0 z + i k_0(\alpha x + \beta y)} \frac{d\alpha d\beta}{U_0} \\ \Pi_m = \dfrac{P}{4\pi^2} \displaystyle\int \int (\alpha \sin\chi - \beta \cos\chi)\, \tilde{f}_m(U_0)\, e^{-U_0 k_0 z + i k_0(\alpha x + \beta y)} \frac{d\alpha d\beta}{U_0} \end{cases} \tag{16}$$

where

$$\tilde{f}_e(U_0) = \frac{1}{1 + U_0^2} \cdot \frac{U_0 U_1 \operatorname{th}(U_1 k_0 d)}{D_{TM}} \tag{17.1}$$

$$\tilde{f}_m(U_0) = \frac{i}{1 + U_0^2} \cdot \frac{U_0}{D_{TM}} \quad ; \quad U_1 = \sqrt{U_0^2 + 1 - \epsilon_r} \tag{17.2}$$

Substituting these results into (3.1) and (3.2) now yields all the components of $\bar{E}$ and $\bar{H}$.

2.2 Far-Field Approximation

Recall the identity:

$$\int_{-\infty}^{\infty} \int_{-\infty}^{\infty} \exp[-k_0 U_0 |z - z'| + i k_0 \alpha (x - x') + i k_0 \beta (y - y')] \frac{d\alpha d\beta}{U_0} = \frac{2\pi}{k_0} \cdot \frac{e^{-i k_0 r}}{r} \tag{18}$$

where

$$r = [(x - x')^2 + (y - y')^2 + (z - z')^2]^{1/2}$$

$$\simeq r_0 - \frac{x}{r_0} x' - \frac{y}{r_0} y' - \frac{z}{r_0} z' \quad ; \quad \text{for } |\bar{x}'| << |\bar{r}_0|$$

wherein $r_0 = \sqrt{x^2 + y^2 + z^2}$. Defining the directional-cosines as

$$\nu_x = \frac{x}{r_0} \; ; \; \nu_y = \frac{y}{r_0} \; ; \; \nu_z = \frac{z}{r_0}$$

with

$$\nu_x^2 + \nu_y^2 + \nu_z^2 = 1$$

in general, we can postulate that for $(k_0x, k_0y, k_0z) >> 1$,

$$\int_{-\infty}^{\infty}\int_{-\infty}^{\infty} \tilde{f}\,(\alpha,\beta,U_0)\, e^{-U_0k_0z + ik_0(\alpha x + \beta y)} \frac{d\alpha d\beta}{U_0} \simeq \frac{2\pi}{k_0} \tilde{f}\; (\alpha \to \nu_x; \beta \to \nu_y; U_0 \to -i\nu_z) \frac{e^{-ik_0r_0}}{r_0} \qquad (19)$$

Far-field patterns of Π_e and Π_m are derived by applying (19) to the integrals in (16), as

$$\begin{aligned} \Pi_e &\simeq \left(\frac{\eta_0 p}{2\pi}\right) \frac{e^{ik_0r_0}}{k_0r_0} [(\nu_x \cos\chi + \nu_y \sin\chi)\tilde{f}_e(-i\nu_z)] \\ \Pi_m &\simeq \left(\frac{p}{2\pi}\right) \frac{e^{ik_0r_0}}{k_0r_0} [(\nu_x \sin\chi - \nu_y \cos\chi)\tilde{f}_m(-i\nu_z)] \end{aligned} \qquad (20)$$

In order to obtain the far-field expressions for the electric and magnetic fields, we utilize the fact that to the order of $\frac{1}{k_0r_0}$, one can replace the operation $\nabla \times$ by $ik_0\bar{a}_r$ in (1) so that

$$\bar{E} \simeq -k_0^2 [(\bar{a}_r \times \bar{a}_r \times \bar{a}_z)\Pi_e + (\bar{a}_r \times \bar{a}_z)\eta_0 \Pi_m] \qquad (21)$$

$$= \left(\frac{-k_0\eta_0 p}{2\pi}\right) \frac{e^{ik_0r_0}}{r_0} [(\bar{a}_r \times \bar{a}_r \times \bar{a}_z)(\nu_x \cos\chi + \nu_y \sin\chi)\,\tilde{f}_e(-i\nu_z)$$

$$+ (\bar{a}_r \times \bar{a}_z)(\nu_x \sin\chi - \nu_y \cos\chi)\,\tilde{f}_m(-i\nu_z)]$$

The vector products $(\bar{a}_r \times \bar{a}_r \times \bar{a}_z)$ and $\bar{a}_r \times \bar{a}_z$ as well as the directional-cosines can be explicitly expressed in terms of a spherical coordinate system with respect to any axis.

2.2.1 Z-axis as the polar axis

For example, if we choose the reference axis to be the conventional z-axis (Figure 2), we have in the spherical coordinate system $(\bar{a}_r, \bar{a}_{\theta_z}, \bar{a}_{\phi_z})$:

$$\begin{aligned} \nu_z &= \bar{a}_z \cdot \bar{a}_r = \cos\theta_z \\ \nu_x &= \bar{a}_x \cdot \bar{a}_r = \sin\theta_z \cos\phi_z \\ \nu_y &= \bar{a}_y \cdot \bar{a}_r = \sin\theta_z \sin\phi_z \end{aligned} \tag{22}$$

and

$$\begin{aligned} \bar{a}_r \times \bar{a}_r \times \bar{a}_z &= (\bar{a}_r \cdot \bar{a}_z)\,\bar{a}_r - \bar{a}_z = -(\bar{a}_z \cdot \bar{a}_{\theta_z})\,\bar{a}_{\theta_z} \\ \bar{a}_r \times \bar{a}_z &= (\bar{a}_z \cdot \bar{a}_{\phi_z} \times \bar{a}_r)\,\bar{a}_{\phi_z} = (\bar{a}_z \cdot \bar{a}_{\theta_z})\,\bar{a}_{\phi_z} \end{aligned} \tag{23}$$

where $(\bar{a}_z \cdot \bar{a}_{\theta_z}) = -\sin\theta_z$. Insertion of (22) and (23) into (21) results in the two far-zone orthogonal components of $\bar{E}$

$$\begin{aligned} E_{\theta_z} &\simeq -E_0 \sin\theta_z [(\nu_x \cos\chi + \nu_y \sin\chi)\,\tilde{f}_e(-i\cos\theta_z)] \\ E_{\phi_z} &\simeq -E_0 \sin\theta_z\,[(\nu_x \sin\chi - \nu_y \cos\chi)\,\tilde{f}_m(-i\cos\theta_z)] \end{aligned} \tag{24}$$

where $E_0 = \left(\frac{k_0 \eta_0 p}{2\pi}\right) \frac{e^{ik_0 r_0}}{r_0}$. For the special case when $\chi = 0$, i.e., when the dipole is located in the x-direction, the expressions in (24) reduce to:

$$\begin{cases} E^x_{\theta_z} \simeq iE_0 \cos\phi_z \cos\theta_z \dfrac{U_{1\theta_z}}{U_{1\theta_z} - i\,\epsilon_r \cos\theta\, \mathrm{cth}(U_{1\theta_z} k_0 d)} \\ E^x_{\phi_z} \simeq -iE_0 \sin\phi_z \cos\theta_z \dfrac{1}{\cos\theta_z + iU_{1\theta_z} \mathrm{cth}(U_{1\theta_z} k_0 d)} \end{cases} \tag{25}$$

where $U_{1\theta} = -i\sqrt{\epsilon_r - \sin^2\theta}$. The expressions in (25) are identical to those obtained, with a different approach, by Mosig and Gardiol [1].

2.2.2 Y-axis as the Polar Axis

For studying cross-pol level in a linear array, it is convenient to use the corresponding radiation fields expression derived with the polar axis of the spherical coordinates in the array direction, i.e., the y-axis (Figure 3a).

In the spherical coordinate system ($\bar{a}_r$, $\bar{a}_{\theta_y}$, $\bar{a}_{\phi_y}$), we have

$$\nu_y = \bar{a}_y \cdot \bar{a}_r = \cos\theta_y \tag{26}$$

$$\nu_x = \bar{a}_x \cdot a_r = \sin\theta_y \sin\phi_y$$

$$\nu_z = \bar{a}_z \cdot \bar{a}_r = \sin\theta_y \cos\phi_y$$

and after some vector manipulations

$$\bar{a}_r \times \bar{a}_r \times \bar{a}_z = (-\nu_z \nu_y \bar{a}_{\theta_y} - \nu_x \bar{a}_{\phi_y}) \sqrt{1-\nu_y^2} \tag{27}$$

$$\bar{a}_r \times \bar{a}_z = (\nu_x \bar{a}_{\theta_y} - \nu_y \nu_z \bar{a}_{\phi_y}) \sqrt{1-\nu_y^2}$$

Substituting (24) and (25) into (21) yields

$$E_{\theta_y} = -E_0 \sin\theta_y \, [-(\nu_x \cos\chi + \nu_y \sin\chi)\nu_y \, \nu_z \, \tilde{f}_e(-i\nu_z) \tag{28}$$

$$+ (\nu_x \sin\chi - \nu_y \cos\chi)\, \nu_x \, \tilde{f}_m(-i\nu_z)]$$

$$E_{\phi_y} = -E_0 \sin\theta_y \, [-(\nu_x \cos\chi + \nu_y \sin\chi)\nu_x \tilde{f}_e(-i\nu_z)$$

$$- (\nu_\chi \sin\chi - \nu_y \cos\chi)\nu_y \, \nu_z \, \tilde{f}_m(-i\nu_z)]$$

We now examine two special cases which are of importance in the present study.

(i) *Y-directed HED*, i.e., parallel polarization.

Let $\chi = \frac{\pi}{2}$ in (28); we then have

$$\begin{cases} E^{y}_{\theta_y} \simeq E_0 \dfrac{\sin\theta_y \cos\phi_y}{b} [\sin\theta_y \sin^2\phi_y\, C_{TE} + \cos^2\theta_y \cos\phi_y\, C_{TM}] \\ E^{y}_{\phi_y} \simeq -E_0 \dfrac{\sin(2\theta_y)\sin(2\phi_y)}{4b} [C_{TM} - \sin\theta_y \cos\phi_y\, C_{TE}] \end{cases} \tag{29}$$

where $b = 1 - \sin^2\theta_y \cos^2\phi_y$, and

$$\begin{aligned} C_{TE} &= \frac{1}{\sin\theta_y \cos\phi_y + i(\epsilon_r - b)^{1/2} \cot((\epsilon_r - b)^{1/2} k_0 d)} \\ C_{TM} &= \frac{(\epsilon_r - b)^{1/2}}{(\epsilon_r - b)^{1/2} + i\epsilon_r \sin\theta_y \cos\phi_y \cot((\epsilon_r - b)^{1/2} k_0 d)} \end{aligned} \tag{30}$$

(ii) *X-directed HED*, i.e., perpendicular polarization.

Let $\chi = 0$ in (28), then

$$\begin{cases} E^{x}_{\theta_y} \simeq E_0 \dfrac{\sin(2\theta_y)\sin(2\phi_y)}{4b} [C_{TE} - \sin\theta_y \cos\phi_y\, C_{TM}] \\ E^{x}_{\phi_y} \simeq E_0 \dfrac{\sin\theta_y \cos\phi_y}{b} [\sin\theta_y \sin^2\phi_y\, C_{TM} + \cos^2\theta_y \cos\phi_y\, C_{TE}] \end{cases} \tag{31}$$

where C_{TE} and C_{TM} are given by (30).

3. Cross Polarization Level and Co-Polarized Radiation

3.1 Definition of the Cross-Pol Level (CPL)

In accordance with the IEEE Standard Definition of Terms for Antennas [2], we define the cross-polar side lobe level (CPL) as the maximum relative partial dirctivity (corresponding to the cross-polarization) of a side lobe with respect to the maximum partial directivity (corresponding to the co-polarization) of the antenna. Therefore, with respect to the spherical coordinates (r, θ_y, ϕ_y), one can write:

$$\mathrm{CPL} \equiv \frac{|E_{cross}|_{max}}{|E_{CO}|_{max}} \tag{32}$$

where $|E_{CO}|_{max}$ and $|E_{cross}|_{max}$ are, respectively, the maximum values of co-polar and cross-polar fields for a given value of θ_y and as ϕ_y varies from 0 to 180°.

3.2 Co-pol and Cross-pol for a y-directed HED

For a y-directed HED (Figure 3C), i.e., $\chi = \frac{\pi}{2}$, we have

$$\begin{cases} E^y_{CO} = E^y_{\theta_y} \\ E^y_{cross} = E^y_{\phi_y} \end{cases} \tag{33}$$

where $E^y_{\theta_y}$ and $E^y_{\phi_y}$ are given in (29). For the special case of no slab, i.e., as $\epsilon_r \to 1$, we get

$$\begin{cases} E^y_{CO} = -iE_0 e^{ik_0 d \sin\theta_y \cos\phi_y} \sin\theta_y \sin(k_0 d \sin\theta_y \cos\phi_y) \\ E^y_{cross} = 0\,, \end{cases} \tag{34}$$

i.e., we have a zero cross-pol level. Presence of the substrate ($\epsilon_r > 1$) will increase the CPL.

3.3 Co-pol and Cross-pol for a x-directed HED

For a x-directed HED (Figure 3B), i.e., $\chi = 0$, we have

$$\begin{cases} E^x_{CO} = E^x_{\phi_y} \\ E^x_{cross} = E^x_{\theta_y} \end{cases} \tag{35}$$

where $E^x_{\phi_y}$ and $E^x_{\theta_y}$ are given in (31). For the special case of no slab, i.e., as $\epsilon_r \to 1$, one obtains

$$\begin{cases} E^x_{CO} = -iE_0 e^{ik_0 d \sin\theta_y \cos\phi_y} \cos\phi_y \sin(k_0 d \sin\theta_y \cos\phi_y) \\ E^x_{cross} = -iE_0 e^{ik_0 d \sin\theta_y \cos\phi_y} \cos\theta_y \sin\phi_y \sin(k_0 d \sin\theta_y \cos\phi_y) \end{cases} \tag{36}$$

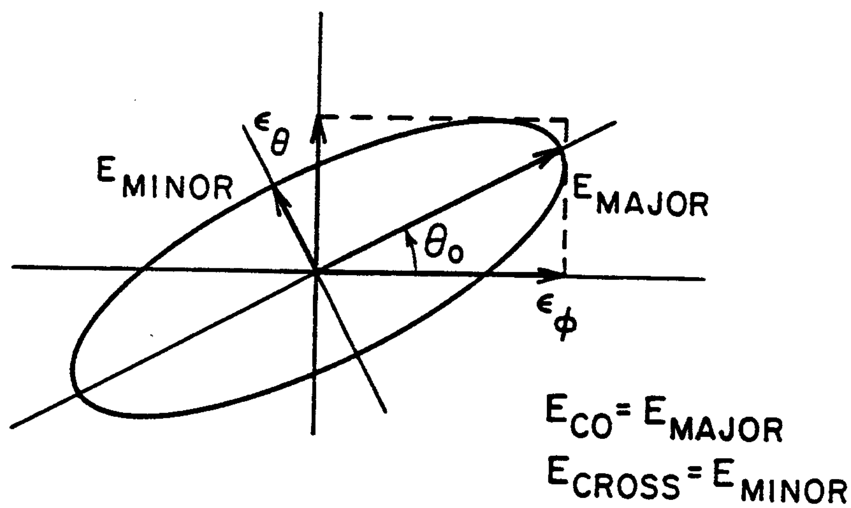

Fig. 4: Elliptical polarization for an arbitrarily-oriented dipol.

$$\theta_0 = \frac{1}{2}\tan^{-1}\left[\frac{2|E_{\theta_y}|\,|E_{\phi_y}|}{|E_{\phi_y}|^2 - |E_{\theta_y}|^2}\cos(\Delta\alpha)\right] \tag{39}$$

where $\Delta\alpha = \alpha_\theta - \alpha_\phi$.

Therefore, provided that the dipole-orientation, χ, is given, one can determine the co-polar direction, θ_0, and the maximum values (maximum with respect to ϕ_y) of E_{CO} and E_{cross}, which are needed to calculate the CPL. Conversely, if a desired co-pol direction of θ_0 and value of the CPL are given, in principle, it is possible to determine the angle χ, i.e., the required orientation of HED.

In deriving the co-polar and cross-polar fields in this work, we have assumed a spherical coordinate with y as the reference axis. However, we note that because the formulation in section 2.2 is in terms of directional cosines ν_x, ν_y and ν_z (see eq. (21)), the discussion is, in fact, independent of the array direction. In other words, one can always assign the dipole-orientation as, say, x and redefine the directional cosines in (21) according to an arbitrary array axis, y'.

4. Numerical Results

For the results presented in this section, the reference-axis (i.e., the array-direction) is assumed to be the y-axis and two cases of diople's orientations are considered.

4.1 y-directed HED

The co-pol ($E_{\theta_y}^y$) and cross-pol ($E_{\phi_y}^y$) radiation patterns for different values of ϵ_r and k_0d are shown in Figures 5-7. The results are normalized with respect to the maximum value of the co-pol, $E_{\theta_y}^y$, which for all the cases considered here occurs at $\phi_y = 0$. As shown, however, the direction of cross-pol's maximum varies depending on the parameters ϵ_r and k_0d.

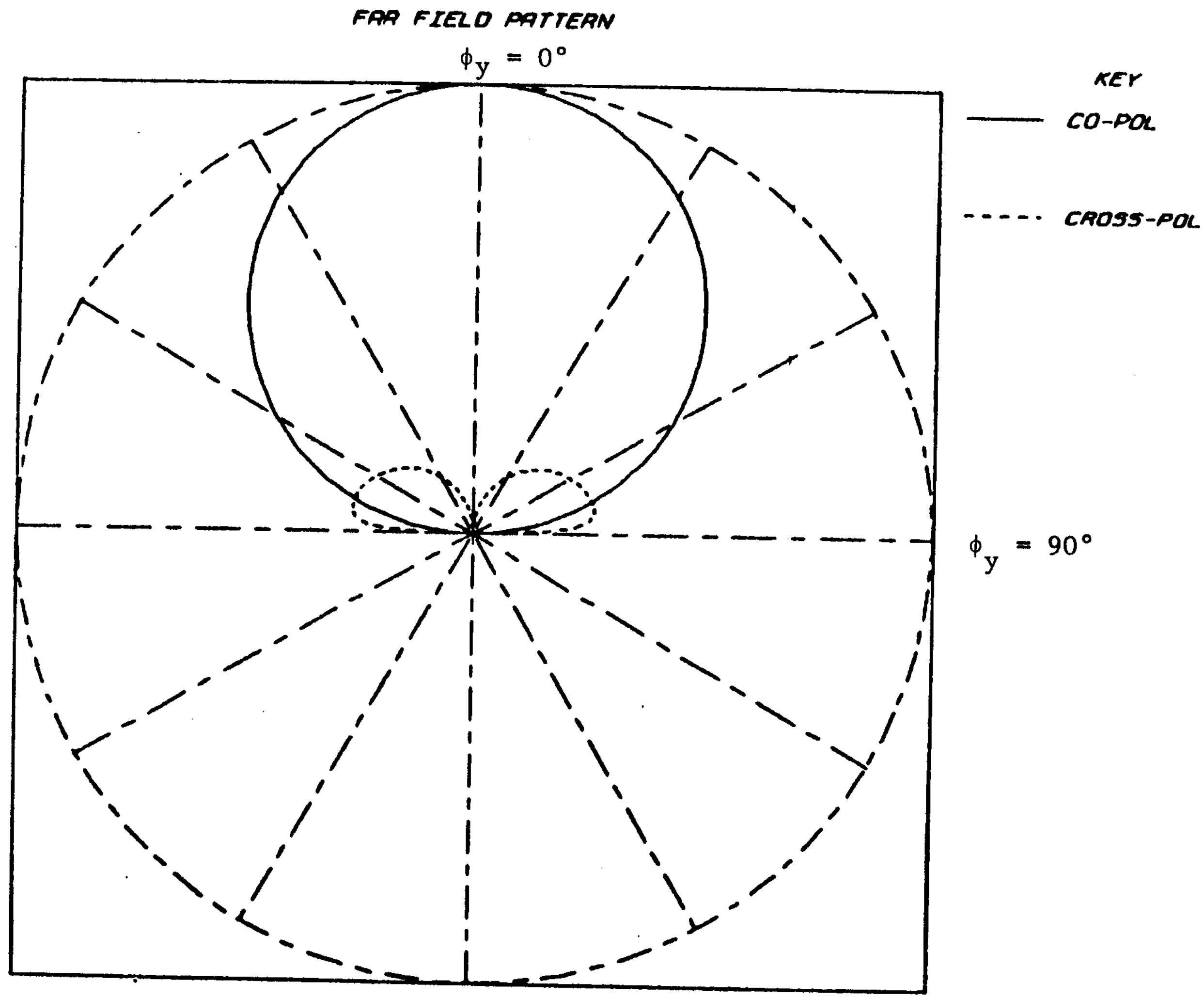

Fig. 5: Co-pol and cross-pol radiation patterns for a Y-directed HED; $\theta_y = 60°$, $\varepsilon_r = 2$, $k_0 d = 0.1$.

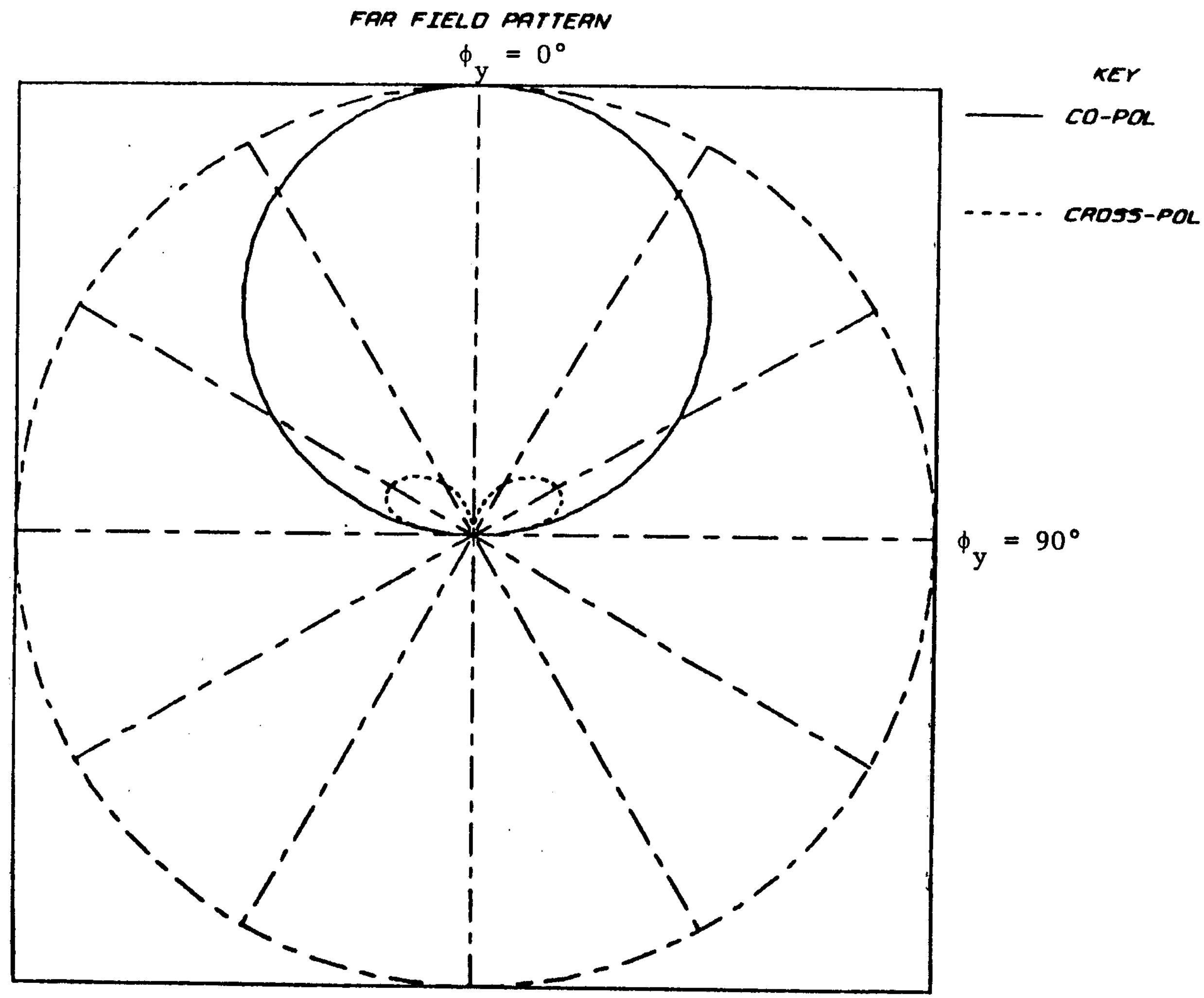

Fig. 6: Co-pol and cross-pol radiation patterns for a Y-directed HED; $\theta_y = 60°$, $\varepsilon_r = 2$, $k_0 d = 0.5$.

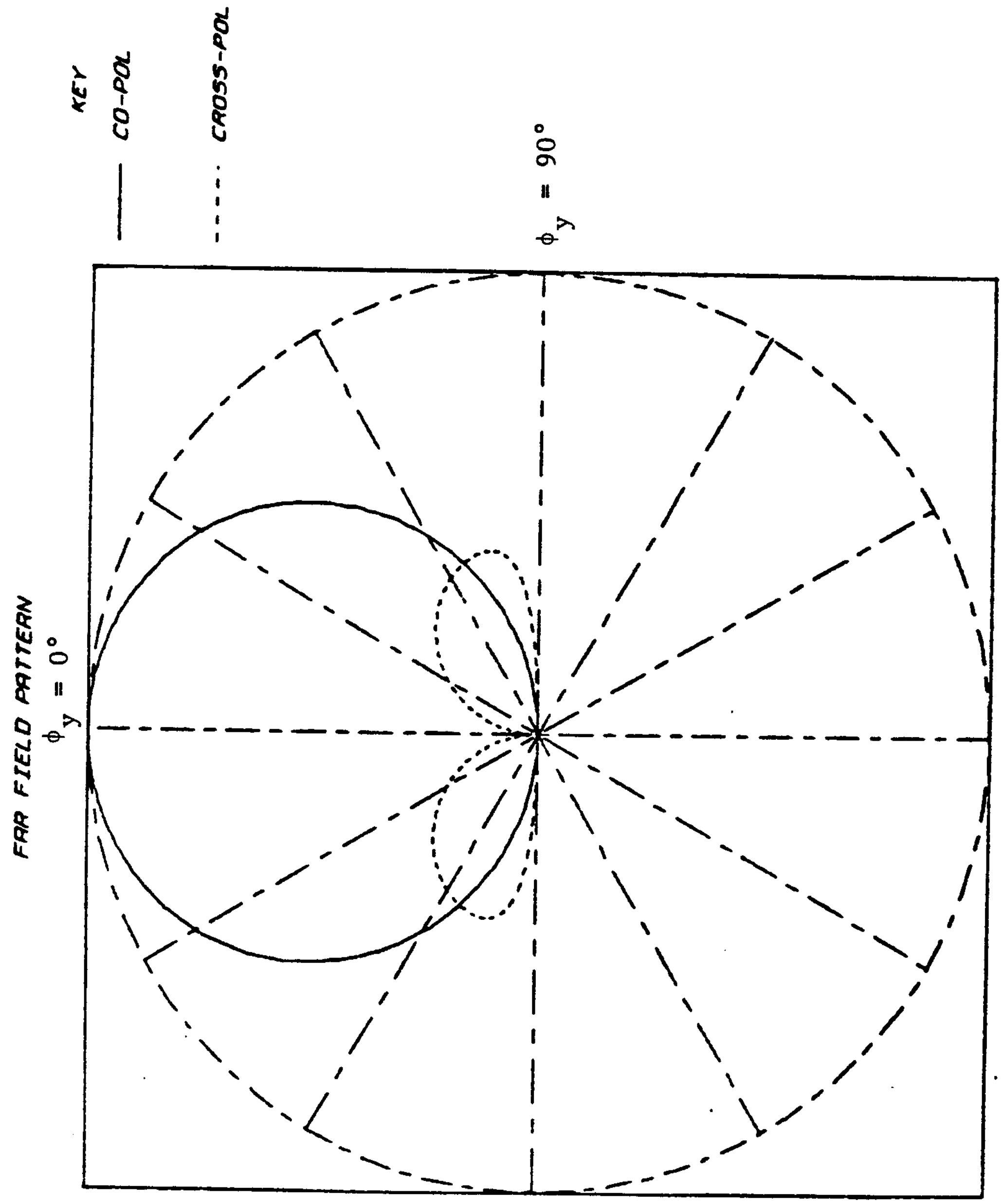

Fig. 7: Co-pol and cross-pol radiation patterns for a Y-directed HED; $\theta_y = 60°$, $\epsilon_r = 10$, $k_0 d = 0.1$.

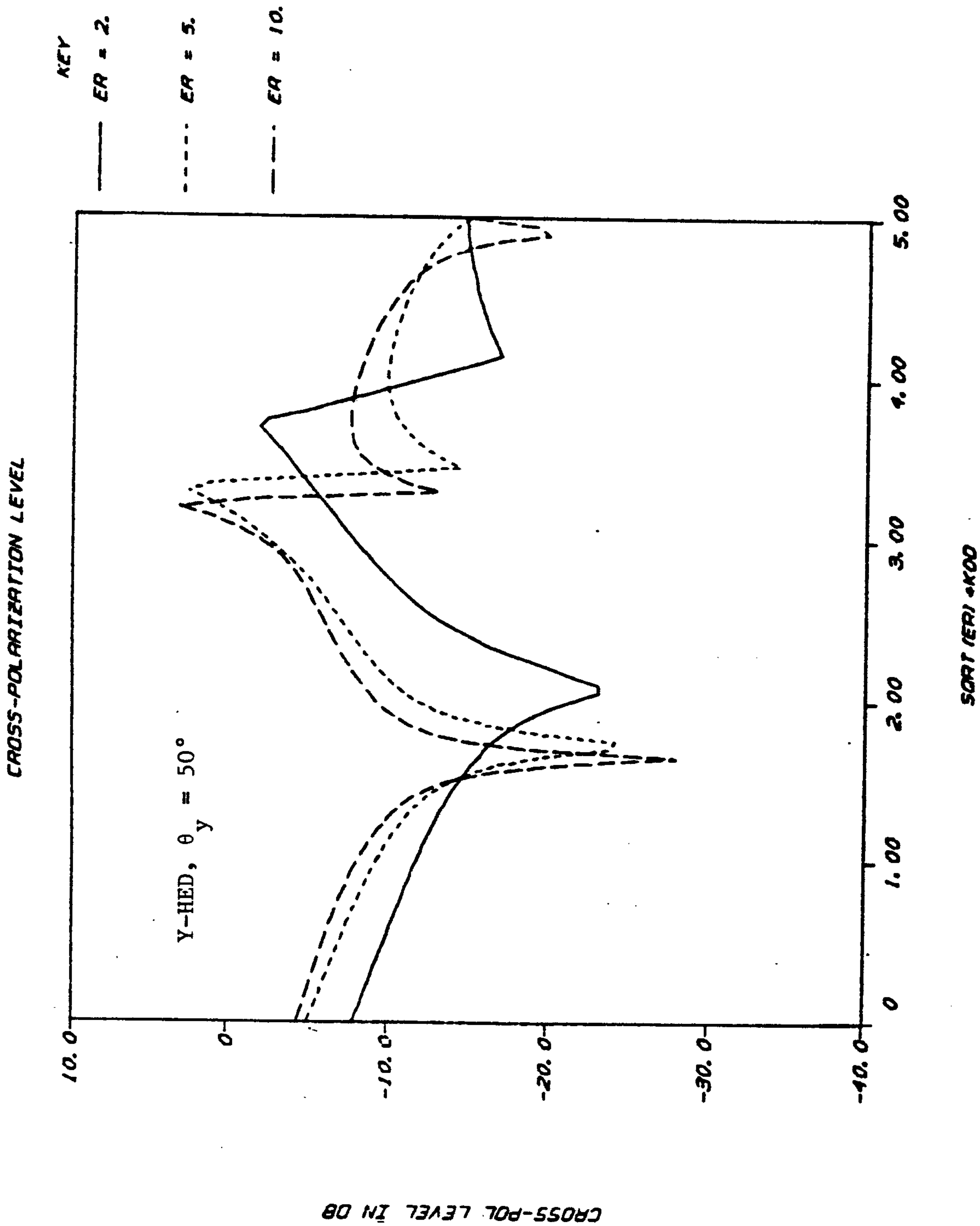

Fig. 8: CPL for a Y-directed HED as a function of $\sqrt{\epsilon_r}\, k_0 d$; $\theta_y = 50°$, $\epsilon_r = 2$, 5 and 10.

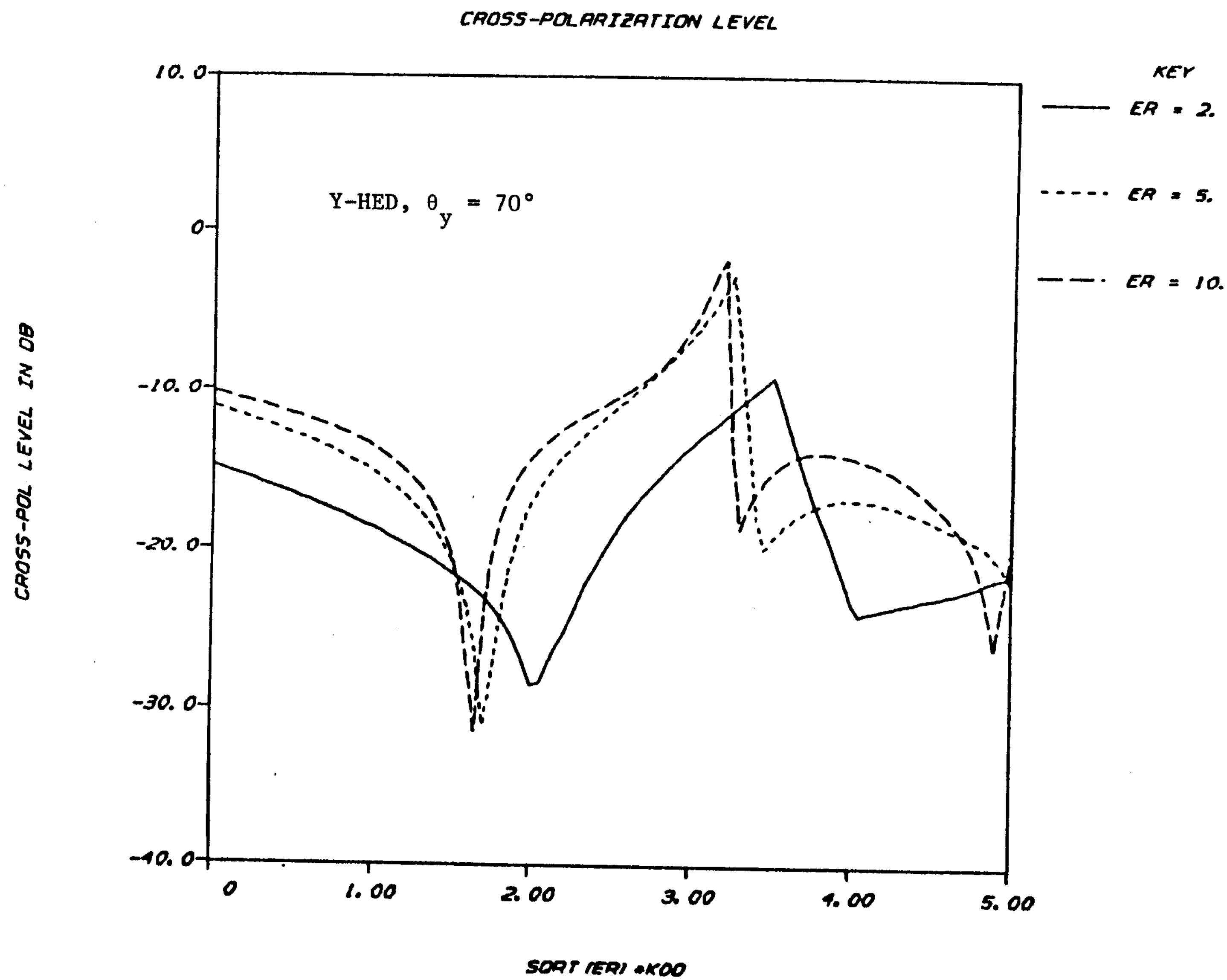

Fig. 10: CPL for a Y-directed HED as a function of $\sqrt{\varepsilon_r}\, k_0 d$; $\theta_y = 70°$, $\varepsilon_r = 2$, 5 and 10.

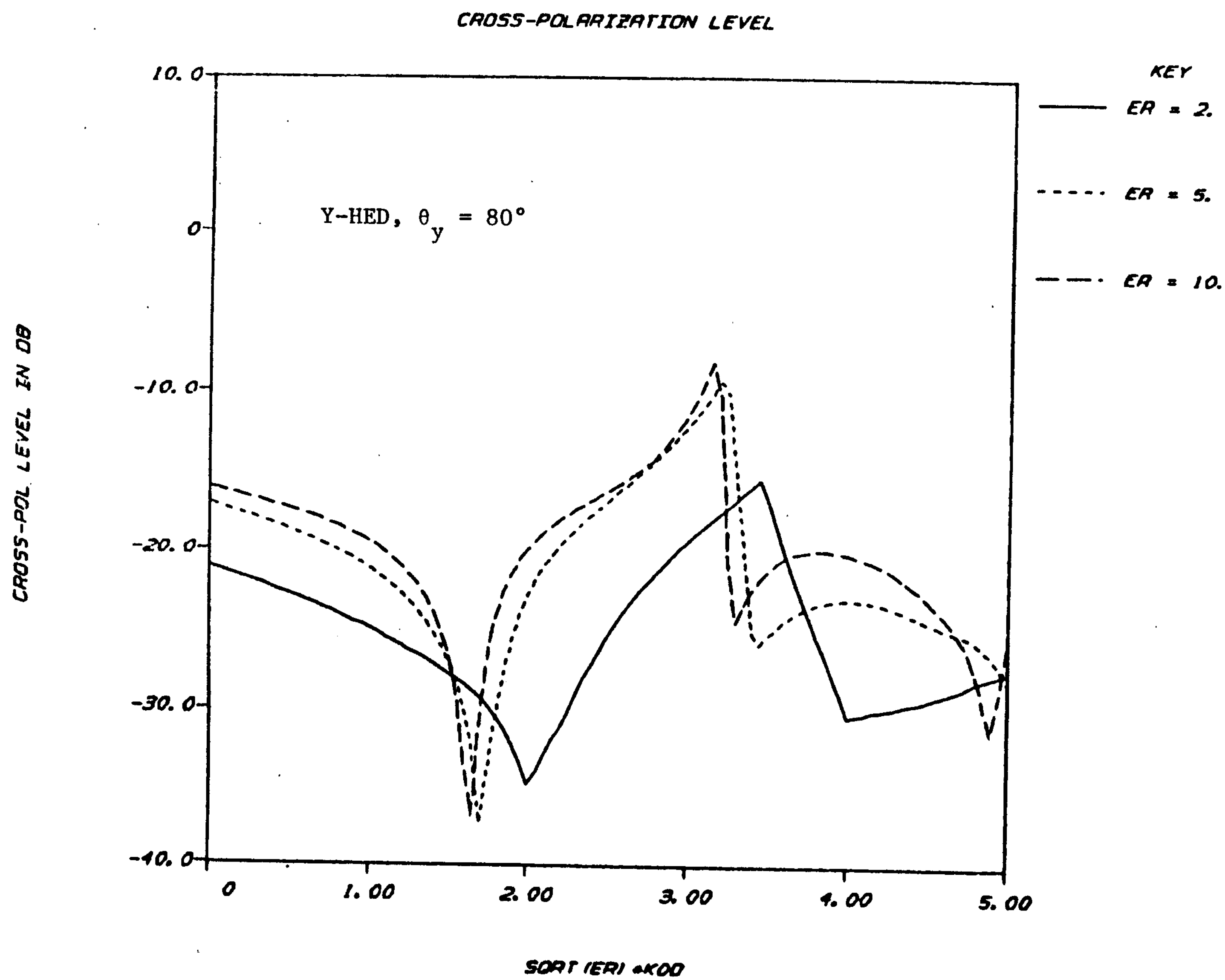

Fig. 11: CPL for a Y-directed HED as a function of $\sqrt{\varepsilon_r}\, k_0 d$; $\theta_y = 80°$, $\varepsilon_r = 2$, 5 and 10.

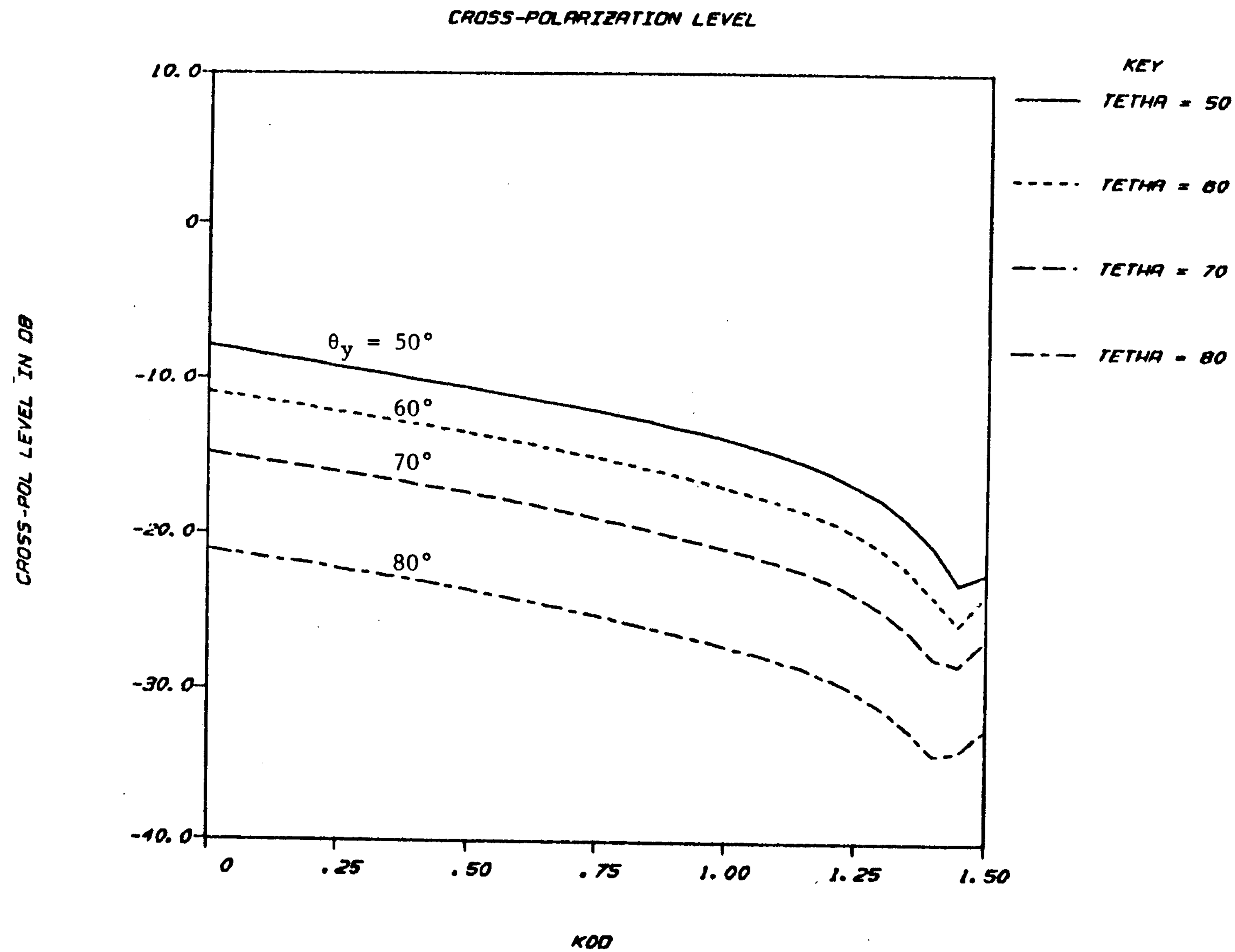

Fig. 12: CPL for a Y-directed HED as a function of k_0d; $\varepsilon_r = 2$, $\theta_y = 50°, 60°, 70°$ and $80°$.

By inserting the values of co-pol and cross-pol's maximums into (32), the cross-pol level is calculated and plotted in Figures 8-11 as a function of k_1d ($= \sqrt{\epsilon_r}\, k_0d$), and for various values of ϵ_r and θ_y. In general, for $0 < k_1d < 1.5$, the cross-pol level (CPL.) decreases linearly as k_1d increases. In addition, the lower the value of ϵ_r, the lower is the CPL. Figure 12 shows the CPL in dB as a function of k_0d and for $\epsilon_r = 2$ and various values of θ_y in degrees. For larger values of θ_y (i.e., closer to broadside direction), the lower values of CPL is achieved. In general, for $k_0d < < 1$, the CPL behaves like (Appendix A)

$$\text{CPL} \equiv \frac{|E^y_{\phi_y}|_{max}}{|E^y_{\theta_y}|_{max}} \simeq \left(\frac{\epsilon_r - 1}{\epsilon_r - \cos^2\theta_y}\right) \cos\theta_y \tag{40}$$

A more accurate expression is given in Appendix A. As expected, for $\theta_y = 90°$, there is no cross-pol radiation and $(\text{CPL})_{dB} \to -\infty$.

These figures show, however, that over the desired range of $50° \leq \theta_y \leq 80°$, no CPL of -30 dB can be achieved for a y-directed HED. We note that because the minimums and maximums in Figures 8-11 correspond to the resonances in the slab and consequently the excitation of surface waevs, all of the values of k_0d larger than that of the first minimum should be avoided. In other words, in order to avoid the higher-order surface modes (other than TM_0 mode that always exists), one should have $k_0d\sqrt{\epsilon_r - 1} < \frac{\pi}{2}$.

4.2 x-directed HED

Figures 13-15 show the co-pol ($E^x_{\phi_y}$) and cross-pol ($E^x_{\theta_y}$) radiation patterns of a x-directed HED over a dielectric slab. The corresponding cross-pol levels are shown in Figures 16-20. As opposed to the y-HED case, the CPL in this case initially incrases with increasing k_1d (see Figures 12 and 20); furthermore, the higher values of ϵ_r yield lower cross-pol levels.

For this polarization, over the desired range of $50° \leq \theta_y \leq 80°$, the -30 dB CPL can be achieved provided that one chooses a large value of ϵ_r ($\epsilon_r \geq 10$) and small values of k_0d. As

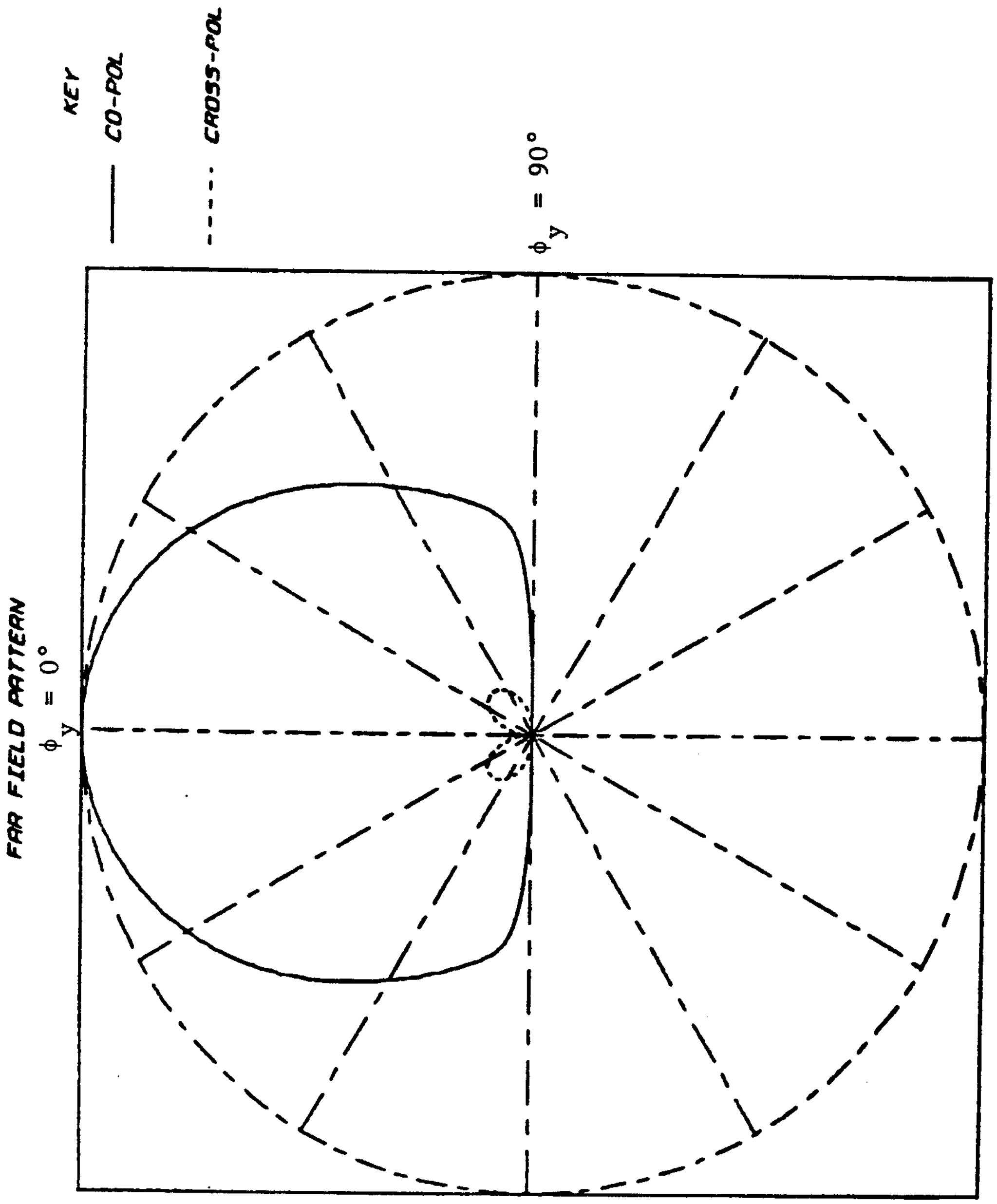

Fig. 13: Co-pol and cross-pol radiation patterns for a X-directed HED; $\theta_y = 60°$, $\epsilon_r = 2$, $k_0 d = 0.1$.

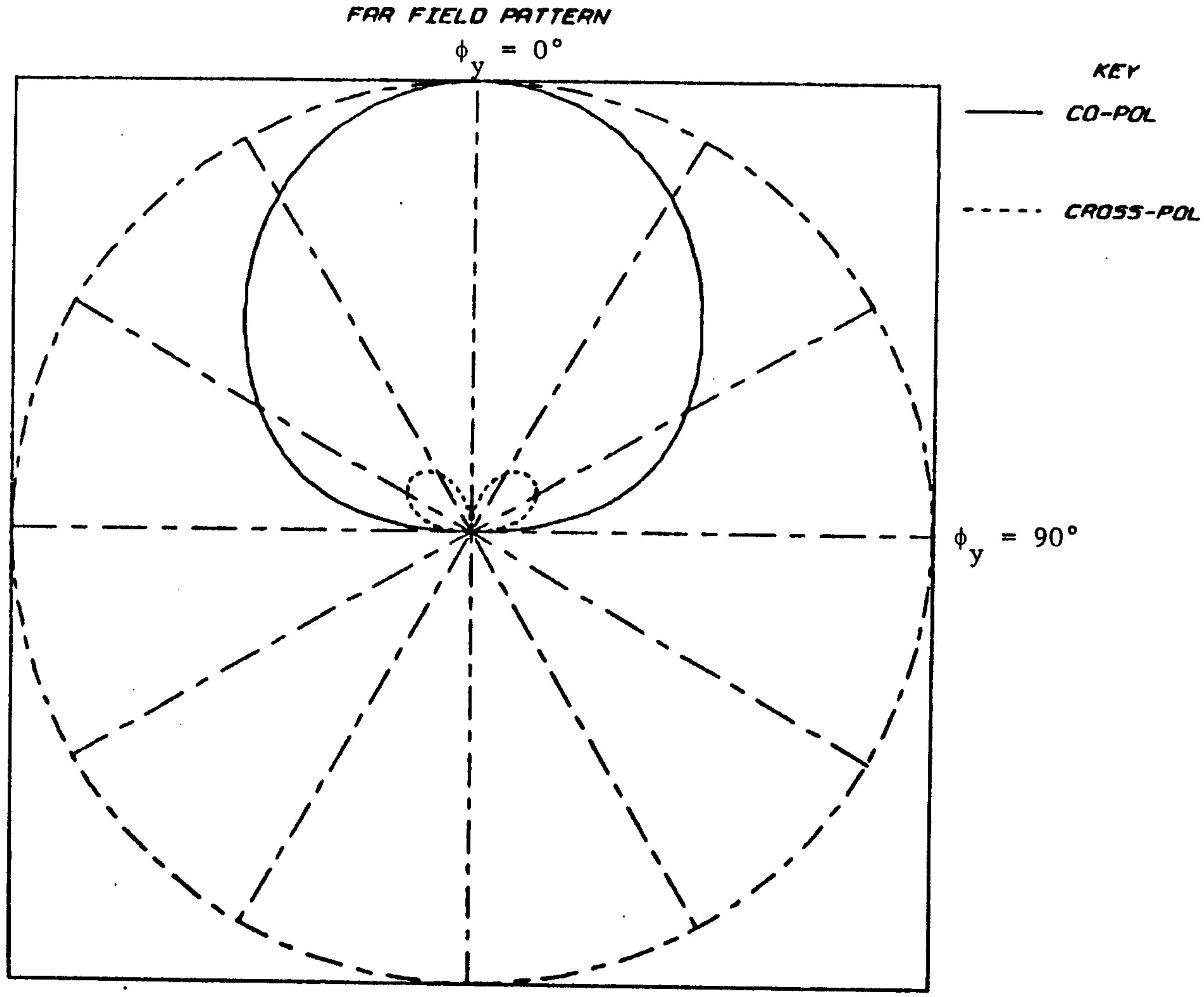

Fig. 14: Co-pol and cross-pol radiation patterns for a X-directed HED; $\theta_y = 60°$, $\varepsilon_r = 2$, $k_0 d = 0.5$.

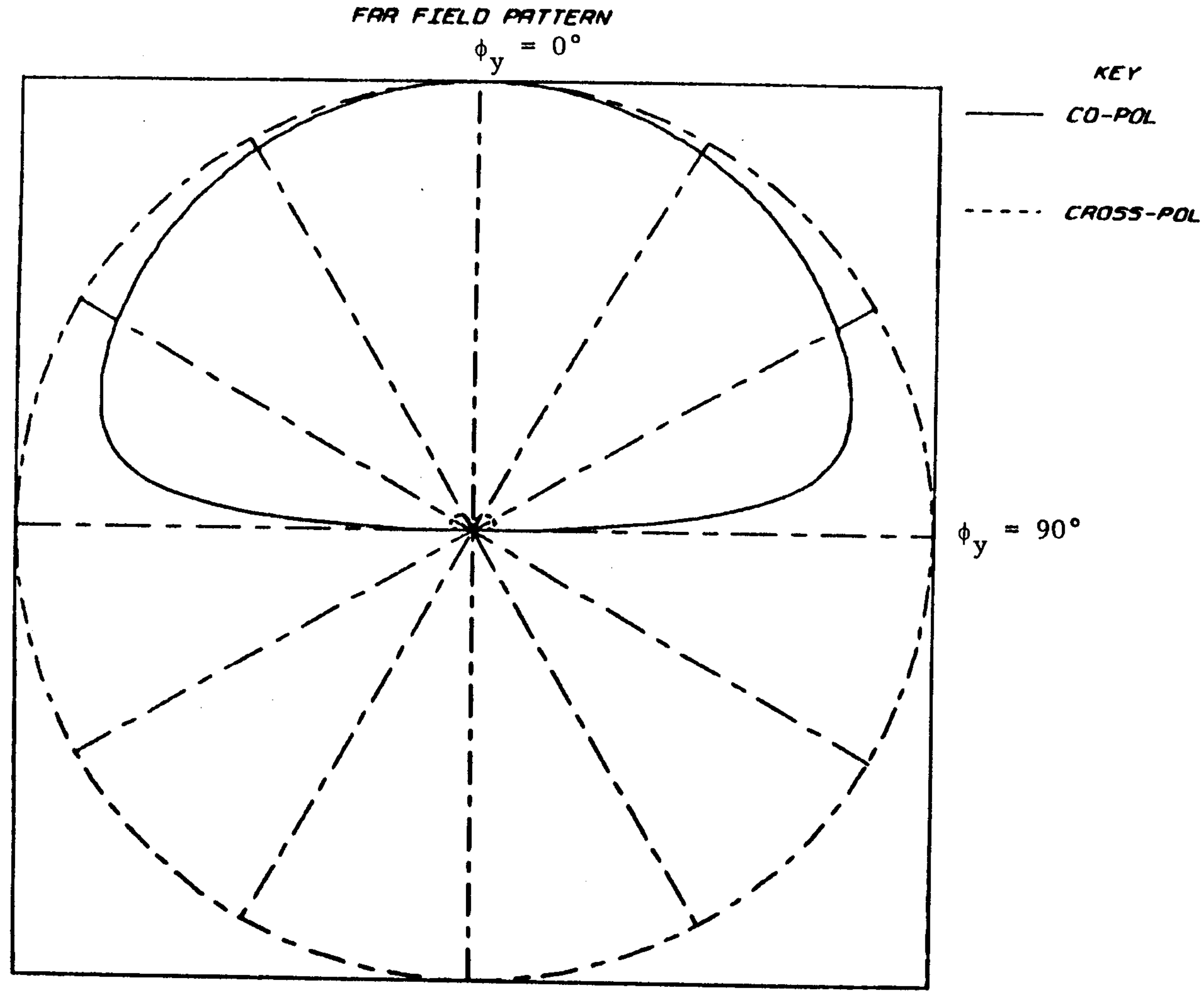

Fig. 15: Co-pol and cross-pol radiation patterns for a X-directed HED; $\theta_y = 60°$, $\varepsilon_r = 10$, $k_0 d = 0.1$.

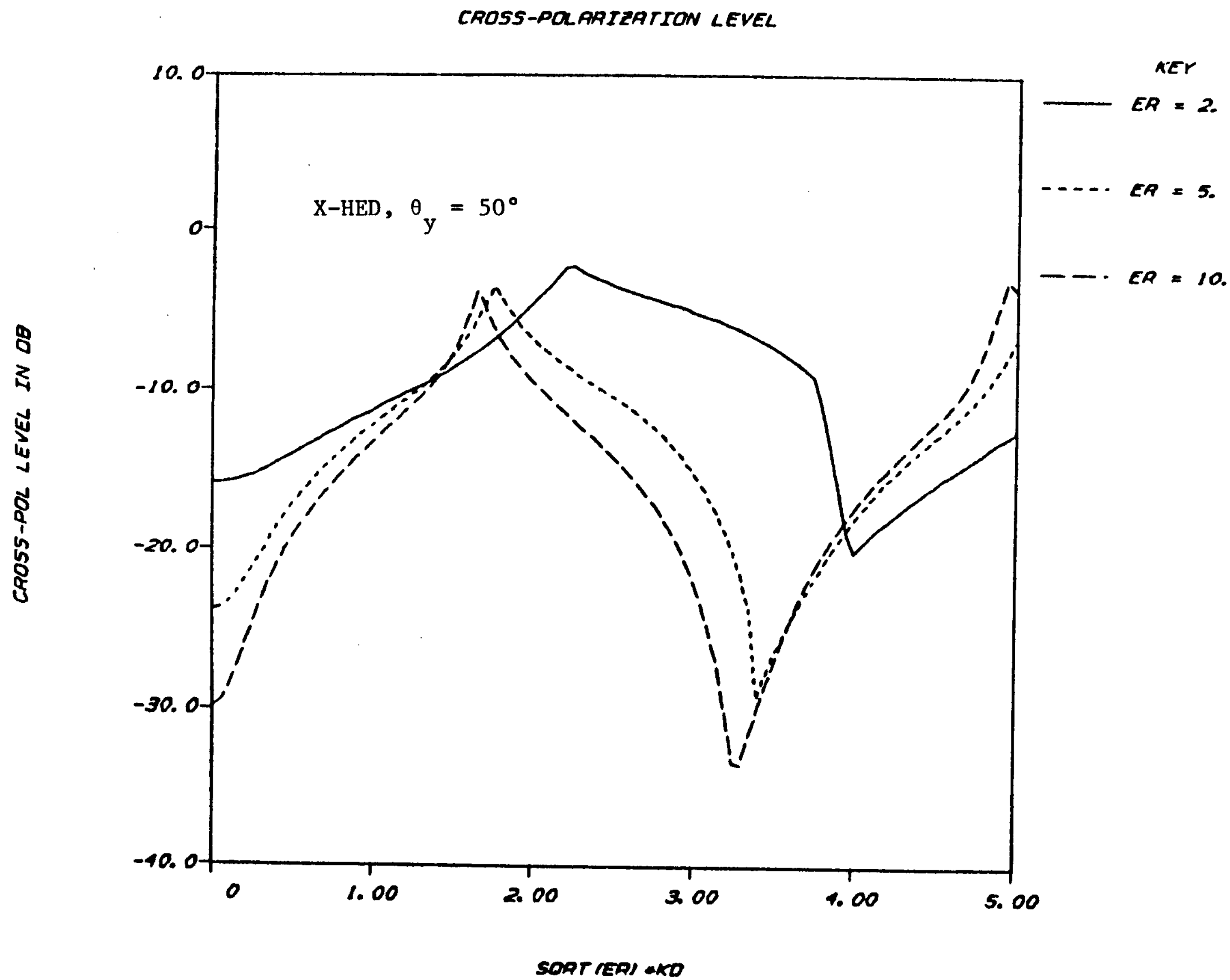

Fig. 16: CPL for a X-directed HED as a function of $\sqrt{\varepsilon_r}\, k_0 d$; $\theta_y = 50°$, $\varepsilon_r = 2$, 5 and 10.

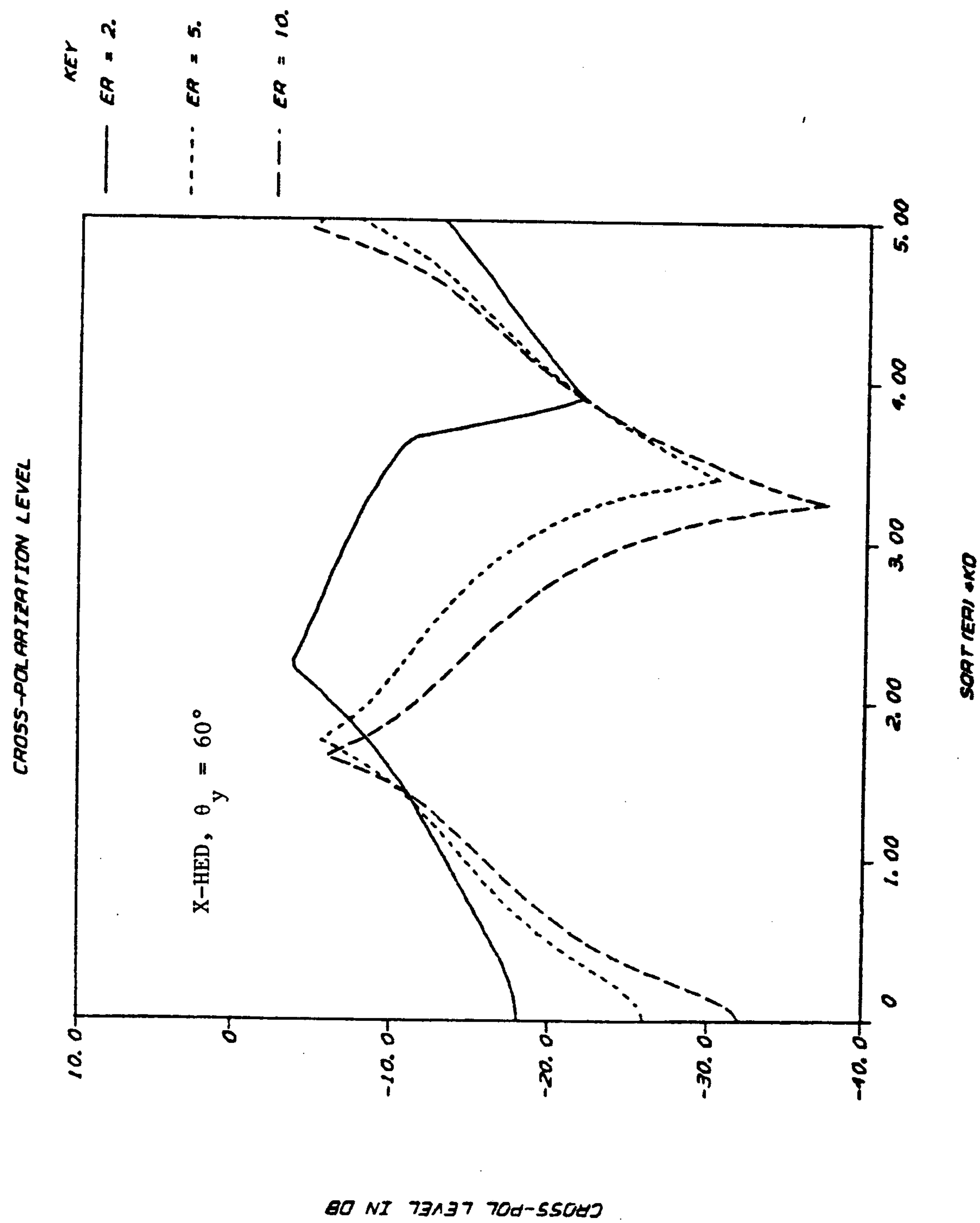

Fig. 17: CPL for a X-directed HED as a function of $\sqrt{\varepsilon_r}\, k_0 d$; $\theta_y = 60°$, $\varepsilon_r = 2$, 5 and 10.

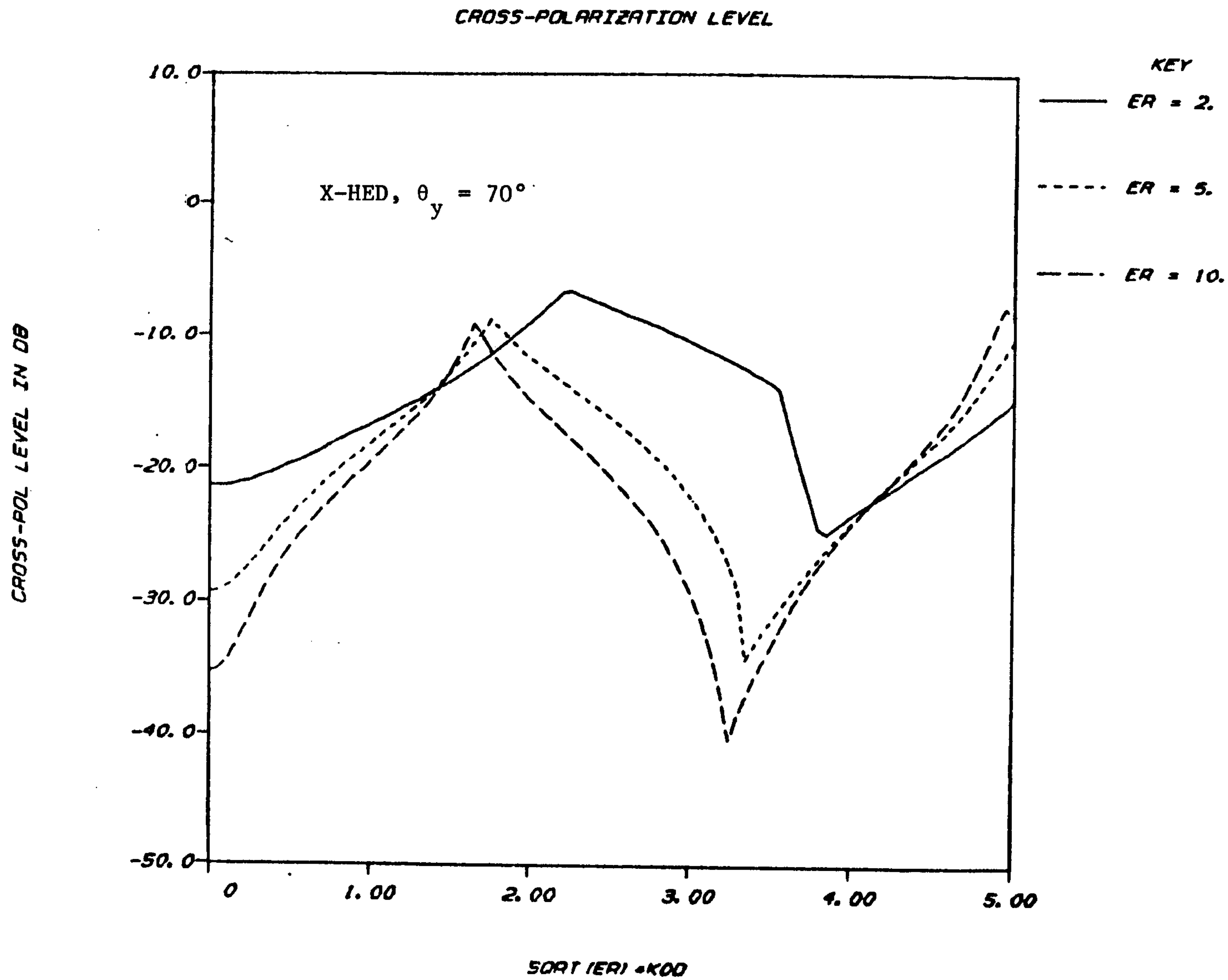

Fig. 18: CPL for a X-directed HED as a function of $\sqrt{\varepsilon_r}\, k_0 d$; $\theta_y = 70°$, $\varepsilon_r = 2$, 5 and 10.

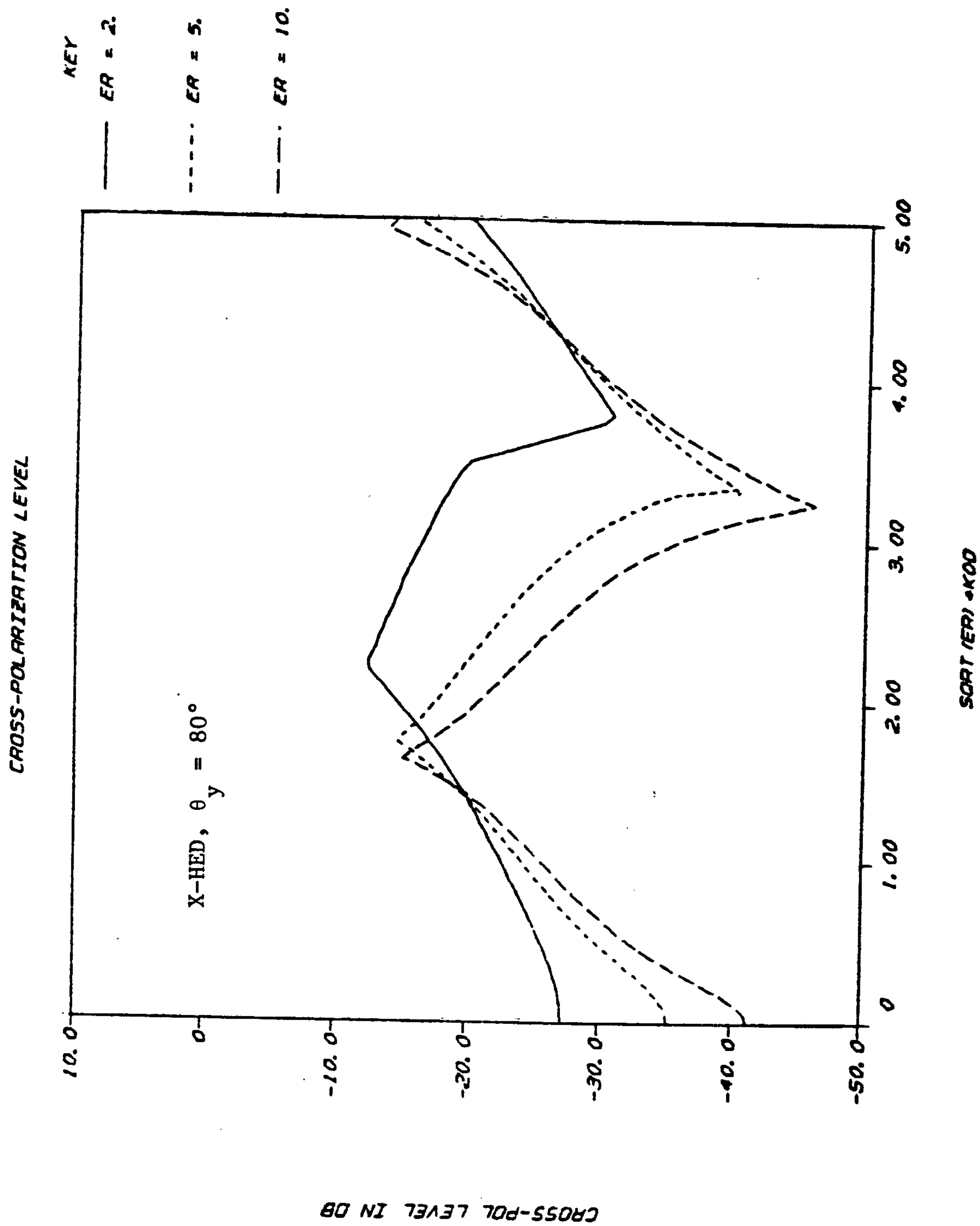

Fig. 19: CPL for a X-directed HED as a function of $\sqrt{\varepsilon_r}\, k_0 d$; θ_y = 80°, ε_r = 2, 5 and 10.

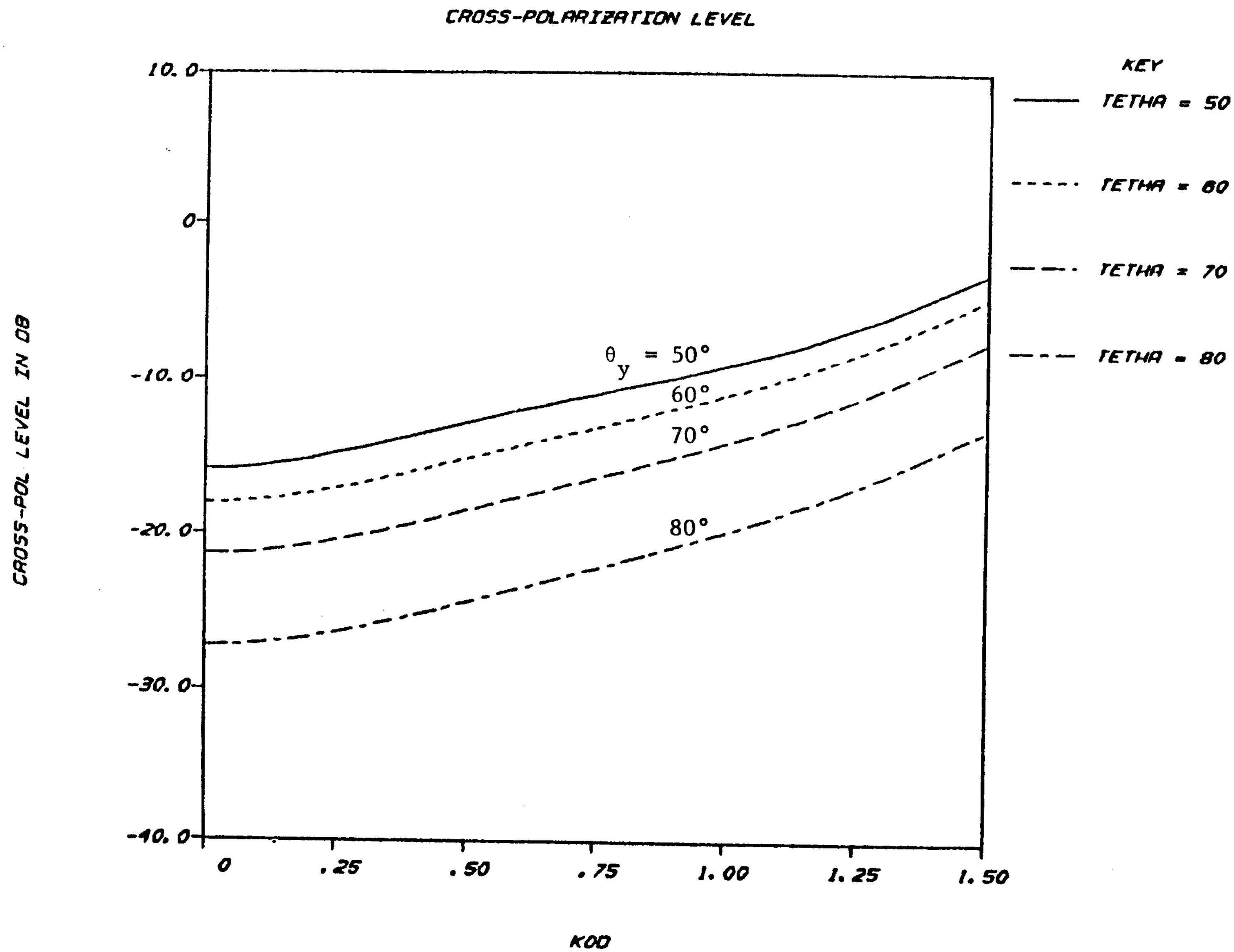

Fig. 20: CPL for a X-directed HED as a function of k_0d; $\varepsilon_r = 2$, $\theta_y = 50°$, 60°, 70° and 80°.

derived in Appendix A, for $k_0d << 1$ and $\epsilon_r >> 1$, the CPL for the x-directed HED behaves like

$$CPL \equiv \frac{|E^x_{\theta_y}|_{max}}{|E^x_{\phi_y}|_{max}} \simeq \frac{k_1 d}{\sqrt{\epsilon_r}} \cot \theta_y \tag{41}$$

5. Conclusions

Expressions for the co-pol and cross-pol fields for any arbitrarily dipole-orientation and array-direction have been derived. These are given by equations (21), (25) and (28)-(31).

It is found that for a y-directed HED a relatively low cross-pol level may be achieved by using small values of ϵ_r and $k_0d\sqrt{\epsilon_r - 1} < \frac{\pi}{2}$. For example, for $\epsilon_r = 2$, $k_0d = 1$ and over the desired range of the beam-direction, $50° \leq \theta_y \leq 80°$, one gets: $-12dB \lesssim CPL \lesssim -25dB$ (see Figure 12). To obtain lower CPL, smaller values of ϵ_r must be used.

For the x-directed HED, however, a -30 dB (or lower) CPL over the whole range of the beam-direction can be achieved by using a large value of ϵ_r (i.e., $\epsilon_r \gtrsim 10$) and a small value of k_0d (Figures 16-19).

In general, the cross-pol radiation cannot be completely eliminated. This stems from the fact that even for the case of an air-filled (i.e., $\epsilon_r = 1$) microstrip (x-directed) dipole antenna, the cross-polarized field (as defined by (36)) always exists. The effect of the dielectric substrate ($\epsilon_r > 1$), as compared to the case of $\epsilon_r = 1$, is to increase the cross-pol level in the y-directed HED and to decrease it in the x-directed HED configurations.

REFERENCES

[1] Mosig. J.R. and F.E. Gardiol, "A dynamical radiation model for microstrip structures", *Advances in Electronics and Electron Physics*, vol. 59, pp. 139-237, 1982.

[2] *IEEE Standard Definition of Terms for Antennas, IEEE Trans. Ant. Prop.*, vol. AP-31, NO. 6, November 1983.

[3] Harrington, R.F., *Time-Harmonic Electromagnetic Fields*, McGraw-Hill Book Company, 1961, pp. 129-132.

[4] Balanais. C.A., *Antenna Theory: Analysis and Design*, Harper and Row, publishers, New York, pp. 48-51, 1982.

APPENDIX A

In this appendix, we derive the approximate expressions for the cross-pol level (CPL) of a microstrip dipole antenna. These expressions are derived for a y-directed HED when $\sqrt{\epsilon_r}\, k_0 d << 1$ and for a x-directed HED when $\sqrt{\epsilon_r}\, k_0 d << 1$ and $\epsilon_r >> 1$.

(I) Y-directed HED.

From (33) and (29), we have

$$E^y_{CO} = E_0 \frac{\sin\theta_y \cos\phi_y}{b} [\sin\theta_y \sin^2\phi_y C_{TE} + \cos^2\theta_y \cos\phi_y C_{TM}] \qquad (A.1)$$

$$E^y_{cross} = -E_0 \frac{\sin(2\theta_y)\sin(2\phi_y)}{4b} [C_{TM} - \sin\theta_y \cos\phi_y C_{TE}] \qquad (A.2)$$

where $b = 1 - \sin^2\theta_y \cos^2\phi_y$, and

$$C_{TE} = \frac{1}{\sin\theta_y \cos\phi_y + i(\epsilon_r - b)^{1/2} \cot((\epsilon_r - b)^{1/2} k_0 d)} \qquad (A.3)$$

$$C_{TM} = \frac{(\epsilon_r - b)^{1/2}}{(\epsilon_r - b)^{1/2} + i\, \epsilon_r \sin\theta_y \cos\phi_y \cot((\epsilon_r - b)^{1/2} k_0 d)} \qquad (A.4)$$

For $k_1 d = \sqrt{\epsilon_r} k_0 d << 1$, we may write

$$\cot((\epsilon_r - b)^{1/2} k_0 d) \sim \frac{1}{(\epsilon_r - b)^{1/2} k_0 d}$$

and therefore the expressions in (A.3) and (A.4) can be approximated by

$$\begin{cases} C^0_{TE} = -ik_0 d \\ C^0_{TM} = \dfrac{(\epsilon_r - b)k_0 d}{(\epsilon_r - b)k_0 d + i\epsilon_r \sin\theta_y \cos\phi_y} \end{cases} \qquad (A.5)$$

Substitution of (A.5) into (A.1) and (A.2) now yields

$$E^{y}_{CO} \doteq E_0 \frac{\sin\theta_y \cos\phi_y}{b} \left[-ik_0 d \sin\theta_y \sin^2\phi_y + \cos^2\theta_y \cos\phi_y C^{0}_{TM} \right] \tag{A.6}$$

$$E^{y}_{cross} \simeq -E_0 \frac{\sin(2\theta_y)\sin(2\phi_y)}{4b} \left[C^{0}_{TM} + ik_0 d \sin\theta_y \cos\phi_y \right] \tag{A.7}$$

In order to calculate the CPL, we need to have the maximum values of $|E^{y}_{CO}|$ and $|E^{y}_{cross}|$ as ϕ_y varies from 0 to π. We note that $|E^{y}_{CO}|_{max}$, at least for small $k_0 d$, always occurs at $\phi_y = 0$; then from (A.6) one gets

$$|E^{y}_{CO}|_{max} \approx E_0 \left(\frac{\epsilon_r - \cos^2\theta_y}{\epsilon_r} \right) k_0 d \tag{A.8}$$

In deriving (A.8) from (A.6), it is assumed that θ_y is not close to zero; this is indeed consistent with the assumption that $50° \le \theta_y \le 80°$.

To obtain the maximum of $|E^{y}_{cross}|$, we let

$$\frac{\partial |E^{y}_{cross}|}{\partial \phi_y} = 0 \tag{A.9}$$

By neglecting the terms of the order $(k_0 d)^4$ and $(k_0 d)^2 \cos^2\phi_y$ (since, we expect $(\phi_y)_{max}$ to be close to $\frac{\pi}{2}$), (A.9) leads to the equation:

$$Z^2 + 2 \left(\frac{\epsilon_r - 1}{\epsilon_r \sin\theta_y} k_0 d \right)^2 Z - \left(\frac{\epsilon_r - 1}{\epsilon_r \sin\theta_y} k_0 d \right)^2 = 0 \tag{A.10}$$

where $Z = \cos^2\phi_y$. Solving (A.10) for Z, yields

$$Z = \frac{1}{\epsilon_r^2 \sin^2\theta_y} \left\{ -(k_0 d)^2 (\epsilon_r - 1)^2 + \left[(k_0 d)^2 \epsilon_r^2 (\epsilon_r - 1)^2 \sin^2\theta_y + (k_0 d)^4 (\epsilon_r - 1)^4 \right]^{1/2} \right\}$$

or, for $\sin\theta_y$ not very small,

$$\cos^2\phi_y = Z \approx \left(\frac{\epsilon_r - 1}{\epsilon_r \sin\theta_y}\right) k_0 d \left[1 - \left(\frac{\epsilon_r - 1}{\epsilon_r \sin\theta_y}\right) k_0 d\right] \tag{A.11}$$

$$\approx \left(\frac{\epsilon_r - 1}{\epsilon_r \sin\theta_y}\right) k_0 d$$

Also,

$$\sin^2\phi_y = 1 - Z \approx 1 - \left(\frac{\epsilon_r - 1}{\epsilon_r \sin\theta_y}\right) k_0 d \tag{A.12}$$

Substituting for $\cos\phi_y$ and $\sin\phi_y$ from (A.11) and (A.12) into (A.7) finally yields

$$|E^y_{cross}|_{max} \approx E_0 \left(\frac{\epsilon_r - 1}{\epsilon_r}\right) k_0 d \left[1 - \frac{2(\epsilon_r - 1)}{\epsilon_r \sin\theta_y} k_0 d\right]^{1/2} \cos\theta_y \tag{A.13}$$

or to the order of $(k_0 d)^2$,

$$|E^y_{cross}|_{max} \approx E_0 \left(\frac{\epsilon_r - 1}{\epsilon_r}\right) k_0 d \cos\theta_y \tag{A.14}$$

By inserting (A.8) and (A.14) into (32), we finally get

$$(CPL)_y \approx \left(\frac{\epsilon_r - 1}{\epsilon_r - \cos^2\theta_y}\right) \cos\theta_y \tag{A.15}$$

A more accurate expression for CPL can be obtained if one uses the expression in (A.13) for $|E^y_{cross}|_{max}$.

$$(CPL)_y \approx \left(\frac{\epsilon_r - 1}{\epsilon_r - \cos^2\theta_y}\right) \left[1 - \left(\frac{\epsilon_r - 1}{\epsilon_r \sin\theta_y}\right) k_0 d\right] \cos\theta_y \tag{A.16}$$

II. X-Directed HED

From (35) and (31), we have

$$E^x_{CO} = E_0 \frac{\sin\theta_y \cos\phi_y}{b} [\sin\theta_y \sin^2\phi_y \, C_{TM} + \cos^2\theta_y \cos\phi_y C_{TE}] \tag{A.17}$$

$$E^x_{cross} = E_0 \frac{\sin(2\theta_y)\sin(2\phi_y)}{4b} [C_{TE} - \sin\theta_y \cos\phi_y C_{TM}] \tag{A.18}$$

For $\sqrt{\epsilon_r}\, k_0 d << 1$ and $\epsilon_r >> 1$, C_{TE} and C_{TM} in (A.3) and (A.4) can be approximated by

$$\begin{cases} C^0_{TE} \approx -ik_0 d \\ C^0_{TM} \approx \dfrac{k_0 d}{k_0 d + i\sin\theta_y \cos\phi_y} \end{cases} \tag{A.19}$$

Substitution from (A.19) into (A.17) and (A.18) gives

$$E^x_{CO} \approx E_0 \frac{\sin\theta_y \cos\phi_y}{b} k_0 d \left[\frac{\sin\theta_y \sin^2\phi_y}{k_0 d + i\sin\theta_y \cos\phi_y} - i\cos^2\theta_y \cos\phi_y \right] \tag{A.20}$$

$$E^x_{cross} \approx -iE_0 \frac{\sin(2\theta_y)\sin(2\phi_y)}{4b} \frac{(k_0 d)^2}{k_0 d + i \sin\theta_y \cos\phi_y} \tag{A.21}$$

Since the maximum value of $|E^x_{CO}|$ occurs at $\phi_y = 0$, therefore from (A.20) we obtain

$$|E^x_{CO}|_{max} \approx E_0 (k_0 d) \sin\theta_y \tag{A.22}$$

In order to obtain $|E^x_{cross}|_{max}$, we let

$$\frac{\partial |E^x_{cross}|}{\partial \phi_y} = 0 \tag{A.23}$$

this leads to an approximate solution

$$\sin^2\phi_y \approx 1 - \frac{k_0 d}{\sin\theta_y} \tag{A.24}$$

Therefore, from (A.21) and (A.24), for $\dfrac{k_0 d}{\sin\theta_y} << 1$, we get

$$|E^{x}_{cross}|_{max} \approx E_0(k_0 d)^2 \cos \theta_y \qquad (A.25)$$

Substitution from (A.22) and (A.25) into (32), finally yields

$$(CPL)_x \approx k_0 d \cot \theta_y = \frac{k_1 d}{\sqrt{\epsilon_r}} \cot \theta_y \qquad (A.26)$$

where $k_1 = (\epsilon_r)^{1/2} k_0$.